Evaluation Tool For The Thermal Performance of Retrofitted Buildings Using An Integrated Approach of Deep Learning Artificial Neural Networks and Infrared Thermography

Amin Al-Habaibeh[1], Arijit Sen[1] and John Chilton[2]

[1]Innovative and Sustainable Built Environment Technologies Research Group (iSBET)

Nottingham Trent University, UK

[2]Department of Architecture and Built Environment,

University of Nottingham, UK

Abstract

In most countries, buildings are responsible for significant energy consumption where space heating and air conditioning is responsible for the majority of this energy use. To reduce this massive consumption and decrease carbon emission, thermal insulation of buildings can play an important role. The estimation of energy savings following the improvement of a building's insulation remains a key area of research in order to calculate the cost savings and the payback period. In this paper, a case study has been presented where deep retrofitting has been introduced to an existing building to bring it closer to a Passivhaus standard with the introduction of insulation and solar photovoltaic panels. The thermal performance of the building with its improved insulation has been evaluated using infrared thermography. Artificial intelligence using deep learning neural networks is implemented to predict the thermal performance of the building and the expected energy savings. The prediction of neural networks is compared with the actual savings calculated using historical weather data. The results of the neural network show high accuracy of predicting the actual energy savings with success rate of about 82% when compared with the calculated values. The results show that this suggested approach can be used to rapidly predict energy savings from retrofitting of buildings with reasonable accuracy, hence providing a practical rapid tool for the building industry and communities to estimate energy savings. A mathematical model has been also developed which has indicated a life-long monitoring will be needed to precisely estimate the benefits of energy savings in retrofitting due to the change in weather conditions and people's behaviour.

Keywords: Artificial Intelligence; Neural Networks; Building thermal performance; Wall insulation; Infrared thermography; Deep retrofitting.

1. Introduction

With the ongoing increase in the world's population and the use of technology, worldwide energy demand is increasing [1]. However, the reserve of fossil fuel, currently the most common source of energy, is limited. Therefore, it is not only necessary to find alternative, ideally renewable, sources of energy but also it is important to develop strategies for reducing energy consumption, particularly in buildings. The Paris Agreement to mitigate the climate change impact sets the target of keeping the global temperature increase below 2°C of the pre-industrial stage [2] with the aspiration to keep the temperature increase below 1.5°C. Moreover,

the UK Government's Climate Change Act (2008) [3] sets a target of reducing greenhouse gas emissions to 80% of the 1990 level by the year 2050. In view of achieving these targets, the Committee on Climate Change [4] recommended that policies should be implemented to make new buildings highly energy efficient as well as to upgrade existing buildings' thermal insulation. According to the UK Green Building Council [5], the infrastructure industry controls 16% of the UK's total carbon emissions, and 37% of the UK's total carbon emissions are related to the use of infrastructure. Buildings consume 20% of overall energy produced worldwide [6] and in the UK domestic energy consumption is 27.2% of overall energy demand [7]. Space heating and hot water is responsible for 80% of overall household energy consumption [8] and heating of residential buildings in the UK is responsible for about 17% of energy related CO_2 emission [9]. The UK Government is going to adopt strategies for limiting greenhouse gas emissions from the built environment to half of the 1990 level by 2050 [10]. In general, it is more effective to reduce the energy demand than to increase the amount of energy production, both economically and environmentally [11]. Therefore, it is necessary to focus on developing strategies to reduce energy consumption in buildings and, in particular, in existing buildings.

Insulation plays an important role in this case by reducing heat loss through the building elements, and consequently reducing the burning of natural resources, such as gas and coal, for electricity generation [12]. The effectiveness of insulation depends on the climate, type of insulation and material used for insulation. In warm regions, space cooling is the central focus during summer, whereas space heating in winter is the major concern in cold climatic regions. Kim and Moon [13] have found that if the U-value of a wall is decreased from 0.57 W/m^{2}K to 0.14 W/m^{2}K by improving wall insulation, it could reduce energy consumption by 25.5% for space heating in cold climate areas in the USA. However, in warm climate areas in the USA, reduction in energy consumption for cooling due to the similar improvement of wall insulation is around 0.14%. Observing the thermal performance of Irish buildings, Byrne et al. [14] have concluded that cavity wall insulation can reduce heat flux through walls by 50% to 52%; and additional external insulation may reduce the heat flux further by 48% to 60%. In the same way, Lee et al. [15] have observed that insulation significantly reduces energy consumption for heating; however, the reduction in energy consumption for cooling depends on the internal heat gain as highly insulated buildings with limited ventilation tend to overheat in summer. Berger et al. [16] demonstrated that additional external insulation in Austrian buildings increases the cooling energy demand in summer slightly; however, the large reduction in heating energy demand in winter outweighs this. On the other hand, Fang et al. [17] have found that external walls made of hollow bricks and insulated with 30mm extruded polystyrene reduce the energy consumption by 23.5% for air-conditioning compared to uninsulated solid walls in a tropical climate during summer. Derradji et al. [18] also have given evidence of external insulation being more effective in reducing energy consumption for cooling during summer than heating during winter in Algeria. Therefore, it can be concluded that insulation plays an important role in reduction of energy consumption during both hot summer and cold winter periods in almost all climatic regions although, the effectiveness of insulation varies at different climate zones.

Depending on the building's surface where the insulation is applied, it can be classified as external insulation or internal insulation. Kossecka and Kosny [19] have showed that external insulation is more effective than internal insulation in different climate zones in the USA. Kolaitis et al. [20] also have found that buildings with external wall insulation of 80 mm Expanded Polystyrene consume 4% to 10% less energy than buildings with internal insulation of the same thickness and material in the same weather conditions. They have also stated that,

considering the space cooling only, the energy consumption with internal insulation is marginally less than the energy consumption with external insulation of similar thickness. However, for space heating the energy consumption with internal insulation is substantially larger than that with external insulation. On the contrary, Wang et al., [21] have presented that internal insulations are the most suitable type to reduce energy consumption during winter and summer in residential buildings of Chongqing city in China. Reilly and Kinnane [22] also have shown that internally insulated building envelopes of Passivhaus standard consume 10% less energy than that of an external insulated building envelopes of the same standard. Although some researchers [21, 22] got analytical results in favour of internal insulation, it has the drawback of reducing available space inside buildings. Furthermore, considering thermo-physical properties of wall insulation, such as time lag and decrement factor, external insulation has been found to have a better performance than internal insulation and cavity wall [23]. Considering the heat storage property of insulation material, Long and Ye [24] have found that external wall insulation has significant influence on energy consumption conversely, internal insulation has almost no influence in this case. Turning to dynamic insulation, Menyhart and Krarti [25] have demonstrated that dynamic insulation in an external wall is also useful to reduce energy consumption for cooling and heating; however, it is more appropriate in the regions where there is a high temperature fluctuation between winter and summer. Other than wall insulation, floor and loft insulation also assists in reducing energy consumption. Although floor insulation may increase the cooling energy demand during the summer period, it significantly reduces the heating energy demand during winter, and eventually the net energy savings for both heating and cooling is around 5.5 kWh/m^2/year [26].

As part of the available technology, infrared thermography has been successfully used for the last five decades to monitor building's thermal performance [27]. Infrared thermography is a method of identifying heat radiation from any object. According to Stephan Boltzmann's law the net heat transfer due to radiation can be expressed as:

$$E = \varepsilon k (T^4 - T_c^4) \tag{1}$$

Where E is the net heat transfer, ε is the emissivity, k is the Stephan Boltzmann's constant, T is the surface temperature and T_c is the surrounding temperature respectively. The value of k is usually taken as 5.67x10^{-8} W/m^{2}K^4. The assumption for equation (1) is that the object will behave as either a black body for emissivity equal to 1 or a grey body for emissivity less than 1; however, we assume that the object will not behave as a non-grey body. It has been assumed that the emissivity value will be constant within the working temperature range and within the spectral range of the camera, which is 7.5-13 μm [28]. In general, the emissivity of a brick wall, doors and windows ranges between 0.85 to 0.95 [29]; however, the emissivity of a low emission glass window is less than 0.07 [30]. An infrared image of a building can reveal heat losses through the building's envelope. For a given building, if the inside temperature is higher than the outside temperature, there will be a net heat transfer to the outdoor environment in the form of radiation and convection. In the case of a higher outside temperature and lower inside temperature, the mechanism is reversed. The convection heat flux can be quantified by multiplying the temperature difference between surface and environment with the heat transfer coefficient of convection as expressed below [31]:

$$H = \alpha_c (T_s - T_{air}) \tag{2}$$

Where H is the convection heat flux, α_c is the heat transfer coefficient of convection, T_s is the surface temperature and T_{air} is the environmental temperature. An infrared camera captures the infrared radiation emitted from a surface, which is the combination of three emissions namely:

emission from that surface, reflection of the surroundings from the surface and emission form the atmosphere. Combining these three, the surface temperature T_s can be calculated by using the following expression [32]:

$$T_s = \sqrt[4]{\frac{W_{tot} - (1-\varepsilon_s)\tau_{atm}k(T_{ref})^4 - (1-\tau_{atm})k(T_{atm})^4}{\varepsilon_s\tau_{atm}k}} \qquad (3)$$

Where W_{tot} is the total radiation received by the camera, ε_s is the emissivity of the surface, τ_{atm} is the transmittance of the atmosphere, k is the Stephan Boltzmann's constant, T_{ref} is the reflective temperature and T_{atm} is the atmospheric temperature. As the value of τ_{atm} is close to 1, the effect of atmospheric temperature is negligible.

Figure 1: An infrared image of a building in Nottingham UK.

An infrared image of a building in the UK is shown in Figure 1, with clear sky and an average ambient temperature of about -1°C. The areas of higher surface temperatures shown in the image expose the poor quality of wall and window insulation as well as air infiltration between the roof and the walls. Furthermore, the warmer structure of the chimney represents heat losses due to the flow of hot air through the chimney, which may be caused by the flue gas from a gas fire. Infrared thermography has a wide range of applications in buildings and they range from evaluating thermal bridging, air leakage, and missing insulation to detection of hot and cold pipes [33]. It is typically useful for measuring a building's thermal performance even in non-steady conditions [34]. The infrared radiation propagates through air for a short distance and hence, it is easier to measure a building's wall surface temperature than with any other methods [35]. In-situ measurement of building heat dispersion using infrared thermographic is a very simple and useful tool for quick assessment of building's thermal performance [36]. Albatici, Tonelli and Chiogna [37] have argued in favour of using infrared thermography for conducting quick thermal performance surveys of existing buildings prior to adopting an investment policy for energy retrofitting. Al-Habaibeh and Siena [38] have utilised infrared thermography to estimate the energy savings in buildings due to improved insulation. Al-Habaibeh, Medjdoub, and Pidduck [39] have also showed the use of thermography to compare the heat loss through openings of different door designs. Bienvenido-Huertas et al. [40] have used infrared thermography for characterising the thermal performance of a building façade. Furthermore, it could also be used to investigate transient temperature response behaviour over the time [41].

Different Artificial Intelligence (AI) based techniques have been used in the prediction of energy consumption in buildings, and among those methods the Artificial Neural Network

(ANN) is the most widely used one [42]. ANN is a mathematical model that mimics the biological nervous system to process information. It consists of several neurons organised in different layers namely input layer, output layer and one or more hidden layers. The input layer process input data for the network and the output layer delivers the results. The hidden layer(s) are mainly responsible for learning the characteristics of input data and the relationship between inputs and outputs. The neurons are composed of weights, biases and a transfer function. The network learns the desired feature from given training data sets and uses the knowledge later on to process unknown inputs. ANN can be used to predict energy consumption patterns of a pre-retrofitted building to compare the energy savings after retrofitting [43]. In terms of predicting energy consumption due to space heating in commercial buildings, ANN has been found to achieve 94% precision [44]; while for predicating cooling load, it drops down to 90% [45]. Furthermore, using a complex network architecture by combining different types of neural networks, the prediction accuracy of heating energy demand could be as high as 98% [46]. Although there are software available to forecast energy consumption in buildings with reasonable accuracy [42] [43], ANN can provide a simpler solution for prediction with less input data and similar accuracy. For instance, Ben-Nakhi and Mahmoud [47] have used a regression neural network to predict hourly cooling load and found very strong agreement with the prediction made using a building energy simulation software namely ESP-r. In another study for predicting daily energy consumption, Neto and Fiorelli [48] found that ANN can produce very close results to the estimation made by the energy simulation software EnergyPlus. Martellotta et al. [49] have also conducted analogous study to predict hourly energy usage of houses modelled on EnergyPlus software, and in 92% cases , they found ANN's prediction accuracy is over 95%. Similar outcome has been found while comparing the ANN result of cooling load prediction with TRNSYS software [50]. The work of Naji et al [51] has also reinforced the fact that ANN produce close prediction to the estimation made by EnergyPlus software for residential buildings' energy consumption. The advantage of ANN for predicting buildings' energy consumption over the conventional statistical methods is its capability of mapping complex relationship between inputs and outputs without the requirement of any prior knowledge about the input-output relationship [52]. Modelling heat losses through a building's wall contains a non-linear and complex relationship among the parameters. ANN based thermal model is found to have a very good capability of nonlinear fitting in such complex cases [53].

Literature has shown significant success of using ANNs in energy consumption prediction; however, limited research has been found in relation to integrating infrared thermography with neural networks to predict future energy consumption. Therefore, this paper includes a novel research where infrared thermography of a deep retrofitted building is combined with deep learning neural networks to estimate the future effectiveness of wall insulation in terms of energy savings. The key aspects of this research work are:

- Evaluating the thermal wall characteristic of insulated and uninsulated buildings using infrared thermography.
- Estimating energy savings due to retrofitting of a building with wall insulation.
- Predicting future heat losses through walls in insulated and uninsulated buildings using ANN from infrared data and historical weather data.
- Evaluating the performance of ANN against calculated heat losses through walls in insulated and uninsulated buildings.

The next sections of this paper include the methodology of the research work followed by a case study in section 3. Later in section 4 the results of infrared thermography and the ANN

analysis are presented and discussed. The limitation of the study is stated in section 5 followed by the concluding remarks in section 6.

2. Methodology

In this work, a deep retrofitted building in the UK is studied using infrared thermography and temperature sensors to examine the thermal performance of the building due to improved insulation. It is then compared with the thermal performance of a standard building in the same area to estimate the energy savings of the retrofitted building. Figure 2 shows the flow chart of the methodology used for this case study. At the beginning, several infrared images of the retrofitted building are captured to analyse the thermal performance. Infrared images of a nearby non-insulated building are also captured for comparison. FLIR E25 thermal camera is used to capture the infrared images and those images are taken on 28th and 29th March at 11:15 pm and 9:30 am respectively. The ambient temperature values are found to be 9°C and 7°C, and the indoor temperatures are measured at 19° C and 20°C respectively. The early morning (6 am) temperature is found approximately to be 4°C. Then, the wall temperature values are extracted from infrared images of both insulated and uninsulated walls. The total heat dissipated from the external wall surface due to convection and radiation is calculated by combining equations (1) and (2),which is expressed as in equation (4) below [54].
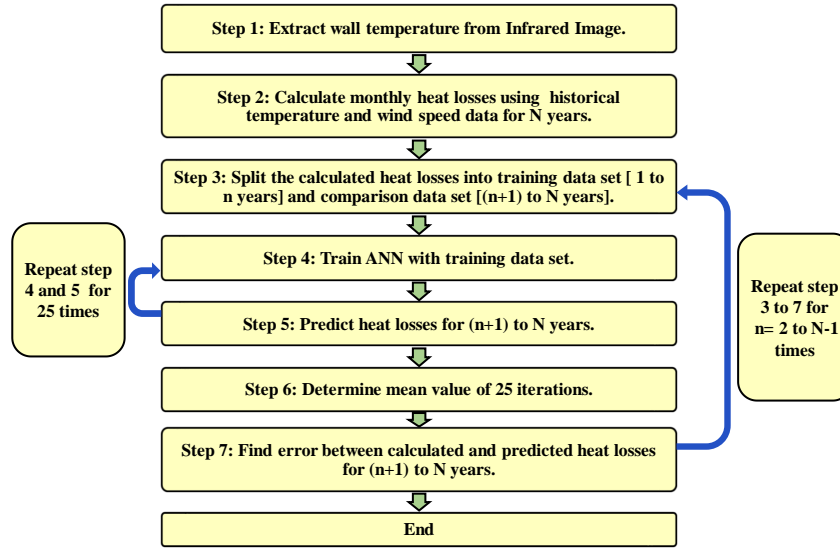

Figure 2: The flow chart of the proposed methodology.

$$P = 5.67\varepsilon_{tot}\left(\left(\frac{T_i}{100}\right)^4 - \left(\frac{T_{out}}{100}\right)^4\right) + 3.8054v(T_i - T_{out}) \quad [\text{W/m}^2] \tag{4}$$

Where P is the total thermal power, ε_{tot} is the emissivity on the entire spectrum, v is the wind speed, T_i is the wall surface temperature and T_{out} is the external environment temperature. The coefficient of convection is replaced with wind speed according to Jurges' equation [54]. Considering a common brick wall, the emissivity value is assumed at 0.93 [55]; and the average wind speed is assumed to be 2 m/s in this case based on past studies [56][38]. If 1W/m^2 heat is radiated for one hour, this will be equivalent to 1Wh/m^2. Therefore, the total heat loss in any given month i through an area of one per square meter of a wall, P_i, can be expressed as:

$$P_i = P \times 24 \times D \qquad (5)$$

Where D represents the number of days in a month. In order to predict future heat losses ANN is used in this paper and the heat losses obtained using equation (5) to validate the prediction. The advantage of ANN is that rather than calculating future heat losses using forecasted temperature in equation (4), the future heat loss can be estimated quickly and thereby eliminating the uncertainty associated with the temperature forecast. The above calculation can be extended to determine monthly heat losses for N years using historical climate data of that locality.

2.1 Optimum number of years to monitor a building

The variation in total heat losses in different years will depend on the variation in weather conditions and occupant's behaviour leading to the question of what should be the optimum number of years (N) a building should be monitored to estimate energy savings.

To address this, let E_i be the energy consumption of a building in a year, where energy consumption can mathematically be expressed as a function of weather and people's behaviour assuming the building characteristic is fixed.

Hence : $E_i = f(w, b)$; where w is the weather condition and b is people's behaviour.

Let, $\sum_1^N E_i$ is the energy consumption over N number of years; hence, the average of annual energy consumption will be $\dfrac{\sum_1^N E_i}{N}$.

If we choose to take another number of years M such that $M = N + k$, where k is an integer and $k \geq 0$; then average of annual energy consumption will be $\dfrac{\sum_1^M E_i}{M}$.

When N reaches its optimum value then the addition of further years will not change the average annual energy consumption; or simply

$$\frac{\sum_1^N E_i}{N} = \frac{\sum_1^M E_i}{M} \qquad (6)$$

Hence $\dfrac{M}{N} = \dfrac{\sum_1^M E_i}{\sum_1^N E_i} = \dfrac{(E_1+E_2+E_3+ \text{............}+E_M)}{(E_1+E_2+E_3+ \text{............}+E_N)} \qquad (7)$

Let, $M = N+k$ where k is the number of additional years, this gives:

$$\frac{N+k}{N} = \frac{(E_1+E_2+E_3+ \text{............}+E_N+E_{N+1}+E_{N+2}+ \text{............}+E_{N+k})}{(E_1+E_2+E_3+ \text{............}+E_N)} = \frac{\sum_1^N E_i + \sum_{N+1}^k E_i}{\sum_1^N E_i} \qquad (8)$$

Simplifying equation (8) leads to:

$$1 + \frac{k}{N} = 1 + \frac{\sum_{N+1}^k E_i}{\sum_1^N E_i} \qquad (9)$$

Subtracting 1 from each side in equation (9):

$$\frac{k}{N} = \frac{\sum_{N+1}^k E_i}{\sum_1^N E_i} \qquad (10)$$

Re-arranging equation (10) leads to:

$$\sum_{N+1}^{k} E_i = \left(\frac{k}{N}\right) \sum_{1}^{N} E_i \qquad (11)$$

Hence from equation (10), as k and N are finite numbers, this makes the equality in the equation is highly unlikely as it is almost impossible to get identical weather condition and occupants' behaviour due to the stochastic and probabilistic nature of the variables to satisfy equation (10).

Since by definition: $\quad \frac{M}{N} = \frac{N+k}{N} \qquad (12)$

If $M \to \infty$ then $N \to \infty$ as k is a constant and hence,

$$\lim_{N \to \infty} \frac{N+k}{N} = \lim_{N \to \infty} \frac{\frac{N}{N} + \frac{k}{N}}{\frac{N}{N}} = \lim_{N \to \infty} \frac{1 + \frac{k}{N}}{1} = 1 \qquad (13)$$

Hence from (12) an (13) this leads to $\frac{M}{N} = 1$ or simply:

$$M = N \qquad (14)$$

From (14) it can be concluded that as long as we have any finite number of years of monitoring the energy consumption of a building, it is not possible to guarantee equality of equation (8) given the changing nature of weather and people's behaviour. Therefore, from equation (8), k should be equal to zero. Hence only infinite number of years to monitor a building is the only guarantee to accurately quantify the energy savings and payback period.

2.2 The implemented approach

The current case study utilises eight years of mean historical temperature data of each month (from 2010 to 2017) extracted from the online sources [57] and [58]. The calculated heat loss data is split into two parts. First part is used for training and validating the ANN model, and the second part is used to compare the difference between ANN prediction and calculated heat losses. The first part of data set is randomly divided as 70% for training, 15% for validation and 15% for testing, which is the suggested settings of training and validation using Matlab software. The ANN predicts monthly heat losses for exactly the same number of years as the second part of data. The training and prediction is repeated for 25 times to avoid overfitting and the mean value of 25 prediction is used to estimate the error. The error and percentage errors are calculated using equation (15) and (16) respectively.

$$e = \sum_{i=1}^{12} (Y_i - P_i) \qquad (15)$$

$$e_p = \frac{e}{\sum_{i=0}^{12} P_i} \times 100\% \qquad (16)$$

Here e is the error, e_p is the percentage error, Y is the ANN predicted heat loss and P is the calculated heat loss from equation (5). To identify the overall performance of the ANN with different training data sets, the whole process of ANN training and prediction is repeated six times by gradually increasing the training data set from two to seven years. As a result, the ANN predicts heat losses for year three to eight. For example, when the ANN is trained with heat losses data from 2010 and 2011, it predicts heat losses for year 2012 to 2017; when the

ANN is trained with heat losses data from 2010, 2011 and 2012, it predicts heat losses for year 2013 to 2017 and so on.
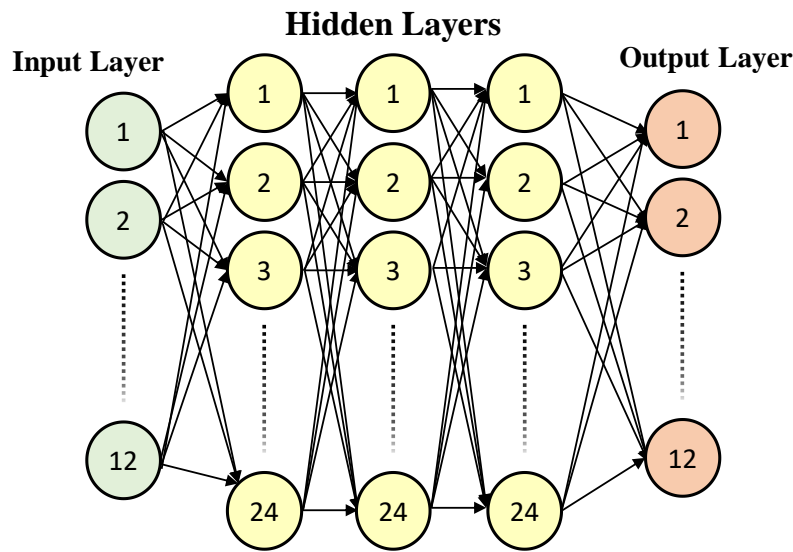

Figure 3: The implemented ANN architecture.

Figure 3 represents the ANN architecture used in this research work. The input and the output layers contain 12 neurons each as the input data set is composed of numerical representation of the months of the year, for several past years, and the output provides the respective heat losses of all those months for future years.
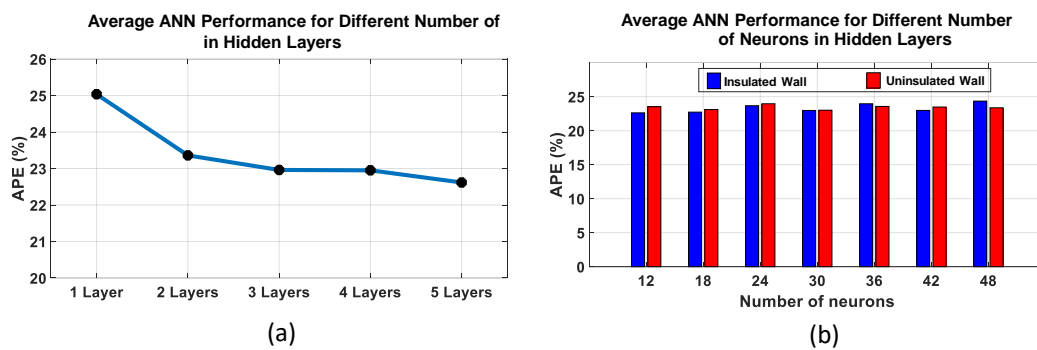

(a)

(b)

Figure 4: The average performance of the ANN with different number of hidden layers and neurons within each hidden layer.

To determine the best architecture of the ANN, the average performance is evaluated using 1 to 5 hidden layers, containing 12, 18, 24, 30, 36, 42 and 48 neurons respectively within the hidden layers. Figure 4-a represents the average performance of the ANN containing 1 to 5 hidden layers and Figure 4-b represents the average performance of the ANN with 12, 18, 24, 30, 36, 42 and 48 neurons respectively in each hidden layer. Absolute Percentage Error (APE) has been considered as the performance measure of ANN which is presented in equation (17).

$$APE = \frac{\sum_{i=1}^{12}|Y_i - P_i|}{\sum_{i=0}^{12} P_i} \times 100\% \qquad (17)$$

The first four years' (2010-2013) data is used to train the network and the following four years' data (2014-2017) is used to evaluate the performance for both insulated and uninsulated walls. As mentioned above, the training and evaluation is conducted 25 times to average the variation in different iterations. It has been found as shown in Figure 4-a, the APE drops significantly in the region between 1 and 3 hidden layers. Then the drop is minor between 3 and 4, then he error is found to improve for the 5 hidden layers ANN. It can be argued that 5 hidden layers could be the best option. However, the calculation time significantly increases in case of four and five layers. Therefore, three hidden layer architecture will be the best compromise in this case. Figure 4-b shows that there is no significant change in APE with the increase of neurons in the hidden layers. However, as the number of neurons in the hidden layers are increased, the calculation time significantly increases. Previous studies have shown that doubling the number of input neurons for the hidden layers would achieve the best performance [59] and [60]. Based on the above analysis and review of past studies, the ANN with three hidden layers and 24 neurons in each layer has been carefully chosen in this study. Hyperbolic tangent sigmoid transfer function is used in the neurons of hidden layer and, Levenberg-Marquardt back-propagation algorithm is used for training the network. In this paper the ANN are used to predict the future thermal performance and equation (4) is used to validate the prediction using real data.

3. The Case Study

An early 19th century house in the UK has been deep retrofitted in accordance with Greening the Box® design concept to reduce the energy cost as well as the dependency on fossil fuel, aiming to minimise greenhouse gas emissions to zero [61]. The location of the house in aerial view is shown in Figure 5-a, and Figure 5-b and 5-c show the plan of the first floor and ground floor. The entrance to the house from the street is on the north-east side. There is a solar photovoltaic array with the capacity of 5.5 kWp on the roof of the house, which consists of nine panels, as shown in Figure 5-a and 6-a.
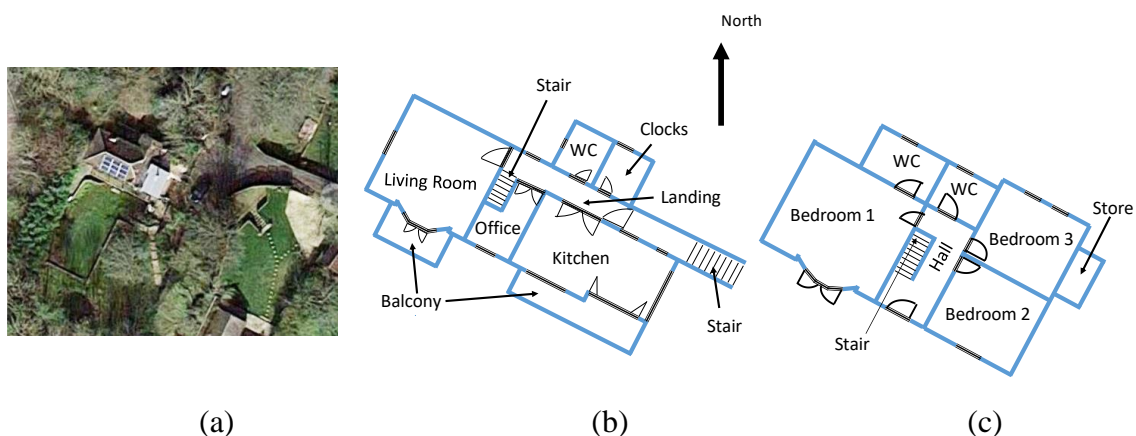

(a)   (b)   (c)

Figure 5: (a) Location of the house and roof top solar panel [source: Google map], (b) First floor layout, (Reproduced from [62]) (c) Ground floor layout.(Reproduced from [63])

As a part of the refurbishment, all bedrooms are relocated to the ground floor; and the kitchen, office and living room are moved to the first floor. The south elevation of the house in Figure 6-a shows that the ground floor of the two-storied building is well below the adjacent street level and the first floor is slightly below street level. Figure 6-b shows the entrance of the house from the east side. The house initially had an oil-fired central heating system which has been replaced with an under floor electric heating system and a wood burning secondary fireplace.

(a)   (b)

Figure 6: (a) South elevation of the house with entrance to the house from street level on the right hand side; (b) house entrance from the east side

The solid walls of the house, before retrofit, had no insulation. To improve the insulation of the building 200 mm thick Styrofoam™A has been externally applied to the external walls as well as underneath the concrete slab of ground floor [61]. Styrofoam™A is an extruded polystyrene foam and has very good insulating capability (R-value circa 6.45 m^2K/W).

200 mm
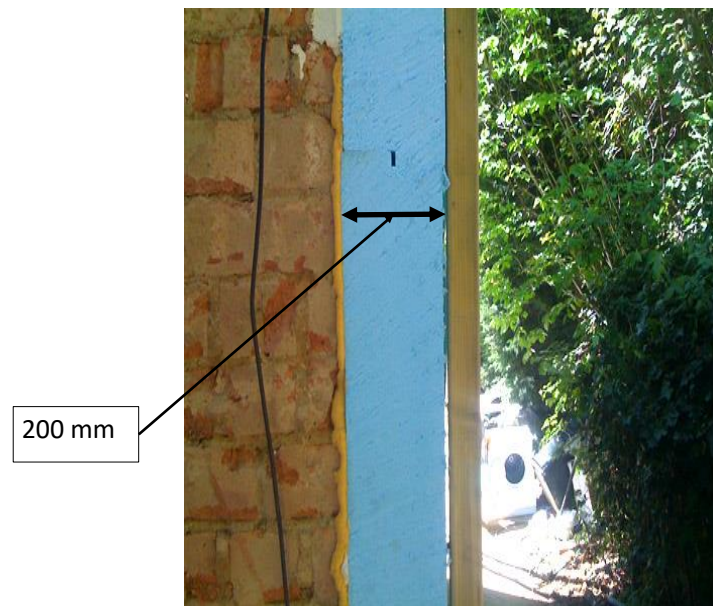
Figure 7: A cross-section in one of the walls showing the external insulation.

The cross section of the original wall brickwork and thickness of new cladding and wood batten holding the cladding in place is shown in Figure 7. The thickness of the solid walls was

approximately 330 mm before refurbishment resulting in a total thickness of over 500 mm post-refurbishment (Figure 8). In order to achieve net positive solar gain, the cumulative window area on the south elevation is increased from 3.9 m² to 9.3 m² and on the north side is reduced from 11.3 m² to 6.1 m² [64]. Therefore, the net glazed area is increased by 0.2 m² which is an increase of only 1.32% from the initial glazed area. All the new windows are fitted with double glazed glass. After retrofitting, the thermal performance of the house is monitored using infrared thermography.

| (a) | (b) | (c) |
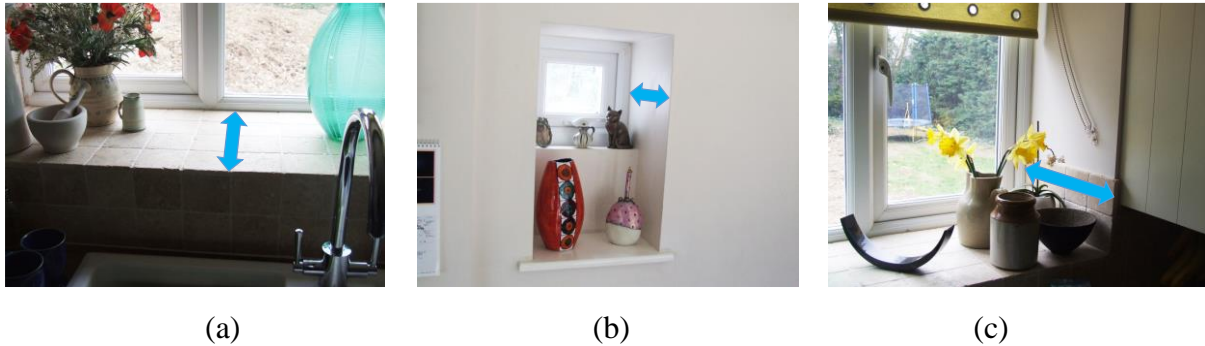
Figure 8: The post-refurbishment wall thickness as seen from the inside.

4. Result and Discussion

4.1 Discussion on infrared thermography result

The infrared images of the building have shown a significant improvement in thermal performance due to the insulation. The visual image (Figure 9-a), and the infrared image (Figure 9-b), taken from the east side of the house, shows the position of a chimney and heat loss through it. The bright colour of the chimney signifies the high heat loss through the chimney with infrared radiation reaching saturation. In contrast, the dark colour of the wall section shows that there is less heat loss through the wall section.
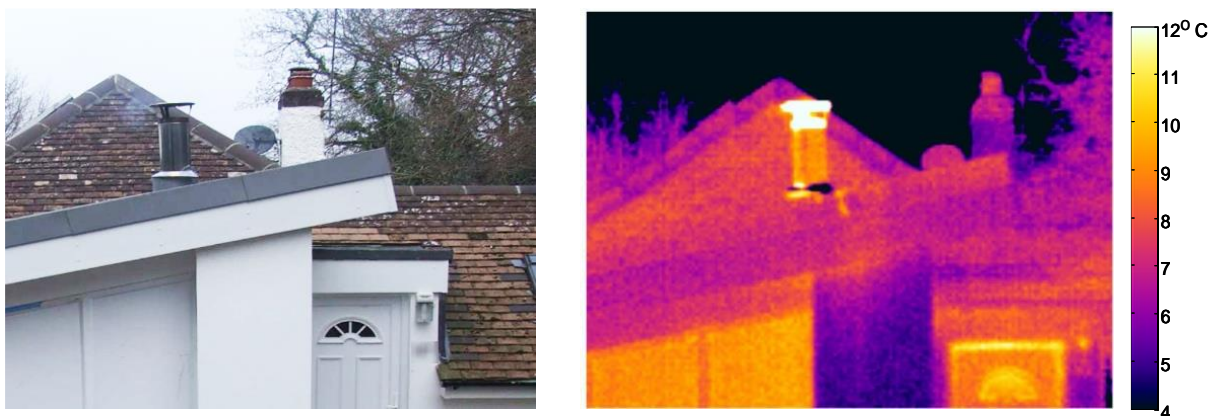

Figure 9: An infrared image showing heat loss through chimney compared to the insulated wall; (a) visual image and (b) infrared image from the east side.

According to the temperature scale on the right hand side of the infrared image, the temperature of the chimney is around 12°C and the temperature of the wall section is around 5°C. However, more detailed analysis shows that the temperature at the top portion of the chimney is about

30.6°C and the temperature of the darkest part of wall is 3.6°C. These discrepancies are due to image saturation.
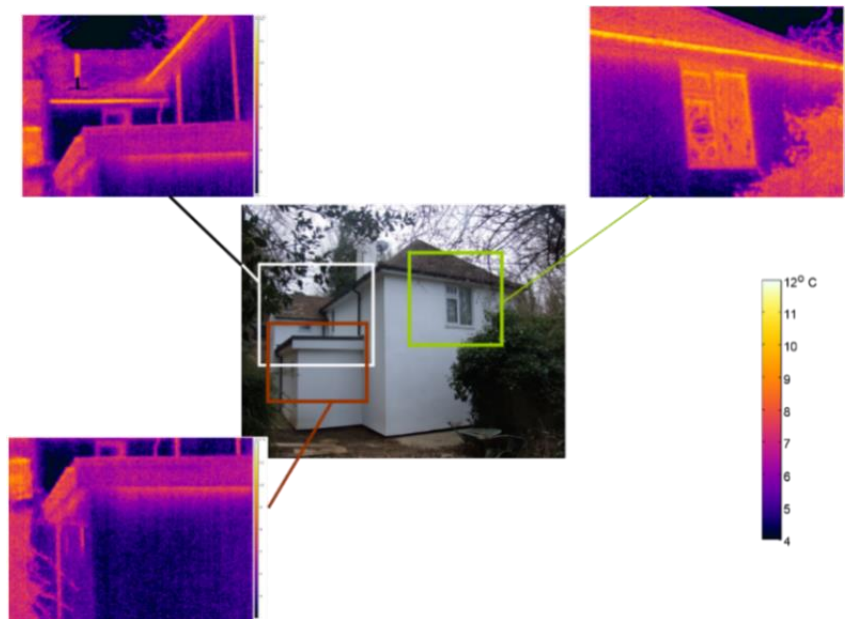

Figure 10: Thermal images of different portions of walls and windows (infrared and visual image from the north-east side).

Figure 10 and 11 show the heat loss through the walls and windows from the north elevation. Different sections on the visual image are shown with rectangular frames and the corresponding infrared image of each section is indicated.
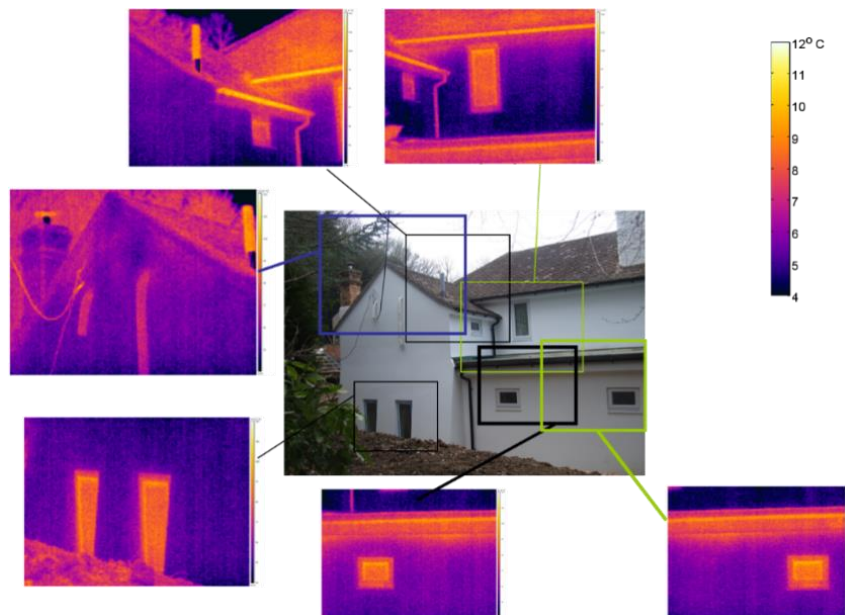

Figure 11: Thermal images of different portions of wall and windows (infrared and visual image from north west side).

The image in Figure 10 is taken from the north-east side of the house and Figure 11 from the north-west. The bright colour of the windows in the infrared images shows the higher heat loss through the windows, and the temperature of the window glazing is about 9°C according to the temperature scale shown on the image. On the other hand, the insulated wall sections are darker

in colour than the windows, which indicates lower heat losses through the wall section. The wall temperature is around 5°C according to the scale shown in Figure 11. Figure 12 includes visual and infrared images taken from the south-east corner of the house, and the infrared image reveals the heat losses through the wall and windows. Again, the bright colour of the windows represents high heat losses and the dark colour of the insulated wall section represents lower heat losses. The temperatures, according to the scale given, of the window and the wall sections are approximately 9°C and 5°C respectively.
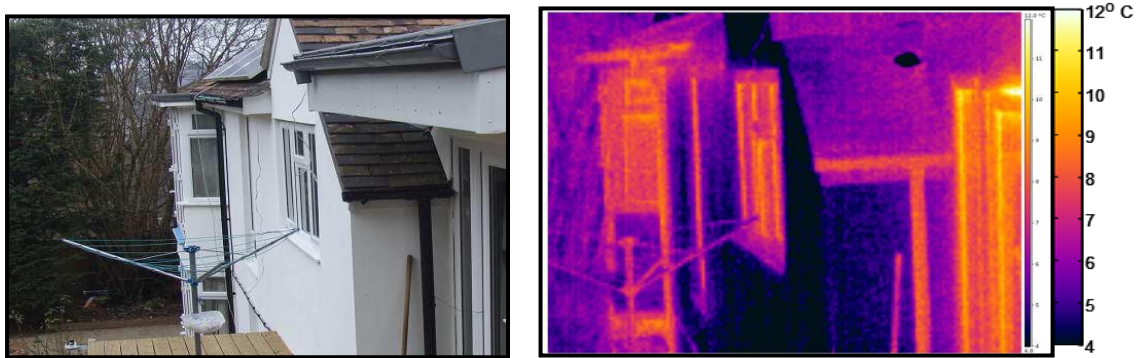
Figure 12: The heat loss through windows (infrared and visual image from south east side).

Figure 13 includes the visual as well as infrared images of different sections of the house taken from the south side. As in the previous infrared images, the high heat losses through the door, windows, gaps around the door frame and chimney are represented in bright colour and the darker colour of the insulated wall sections represent lower heat losses. The temperature of the gap around the door frame is approximately 12°C and the temperatures of the door and window sections are approximately 9°C according the scale shown on the right hand side.
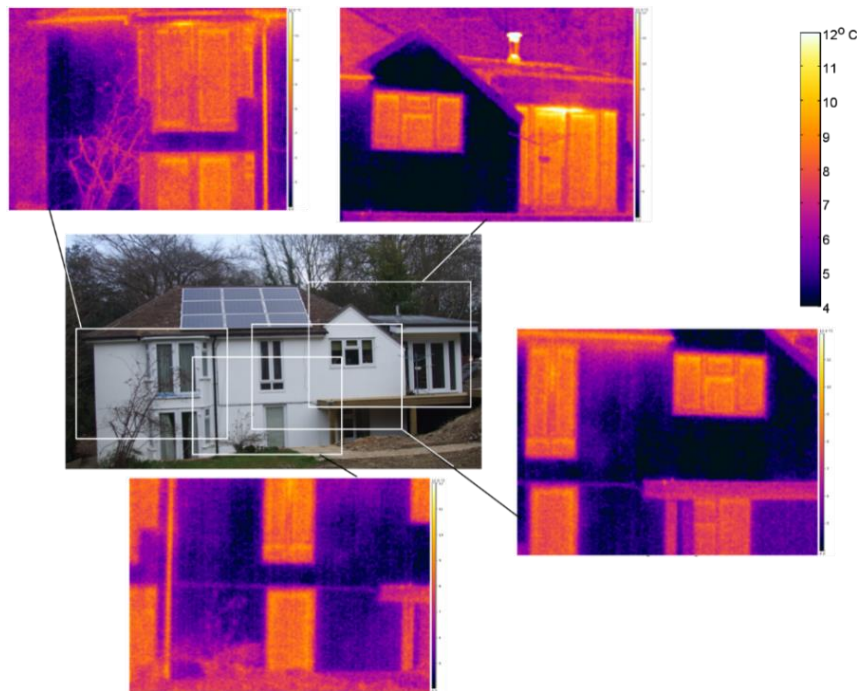

Figure 13: Thermal imaging of different portions of walls and windows (Infrared and Visual image from south side).

The wall temperature varies from 4°C to 5°C, on an average, in different places according to the same scale although the lowest temperature is found to be 3.6°C by the infrared image. Comparing the bright and dark sections of the infrared images and interpreting the respective temperatures from the scale associated with those images it can be clearly recognised that the externally insulated wall significantly reduces heat losses.
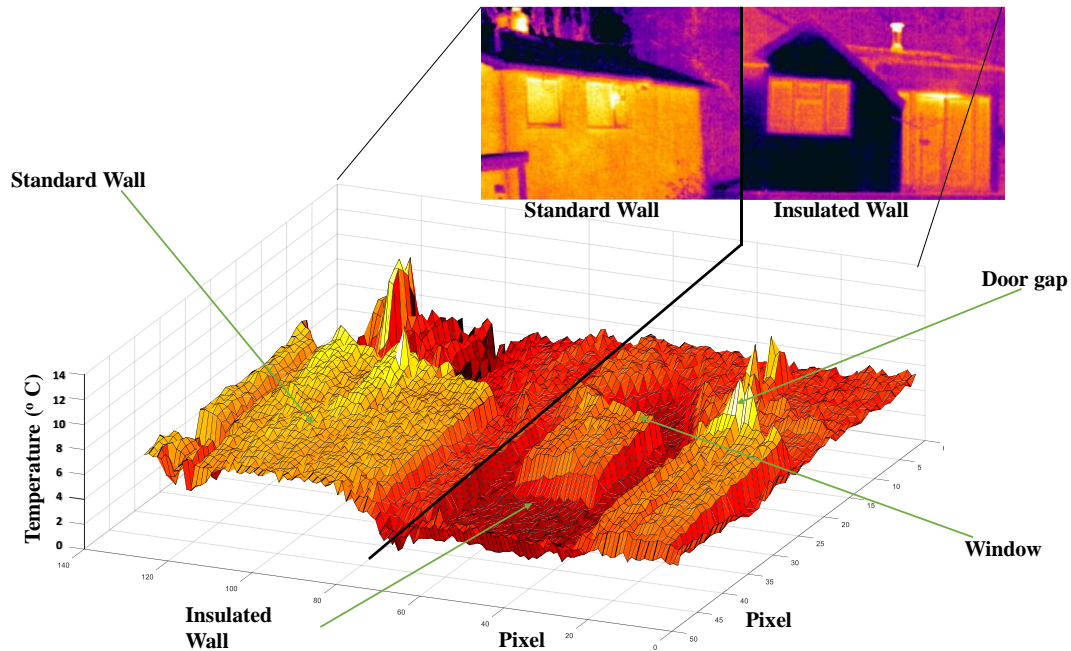

Figure 14: The 3D temperature profile of a standard building versus the insulated deep-retrofitted building.

In order to compare the thermal performance of the insulated wall with that of a wall of similar construction without insulation, the pixel by pixel temperature values are extracted from the infrared images of an uninsulated building and the insulated building. The IR image of the standard building is taken from a nearby building and at the same time as of the retrofitted building. These values are plotted in 3D, next to each other, Figure 14, using Matlab. The temperature profile reveals that the uninsulated wall's surface temperature is around 10°C and the insulated wall's surface temperature is around 4°C. Here the average temperature of all points in the wall sections are considered.

To further distinguish the thermal performance of the uninsulated building and insulated building, the temperature profiles of both walls are constructed along a line as shown in Figure 15. Line AB is constructed on the infrared image containing a section of the standard building and line CD is constructed on the infrared image containing a section of the insulated building. The temperature values at every pixel along the lines AB and CD are extracted using Matlab. These temperature values are then plotted against every pixel. Figure 15 also shows the plotted curve of surface temperature against pixel position along line AB (red) and CD (blue), respectively. The temperature profile of line AB shows that the wall surface temperature mostly remains between 9°C and 10°C. The window-glazed section's temperature is around 11°C. However, there is a sharp rise in temperature between pixels 150 and 200 possibly due to air leakage around a window's opening. The temperature of that portion is 14°C; and it is assumed that the wall sections are homogenous and hence the average wall temperature is considered. Comparing with the early morning ambient temperature (4°C) it is clear that the wall and the

window of the standard building are radiating more heat. Conversely, wall surface temperature of the insulated building, which is close to ambient temperature, establishes the fact that there are very minor heat losses through the wall.
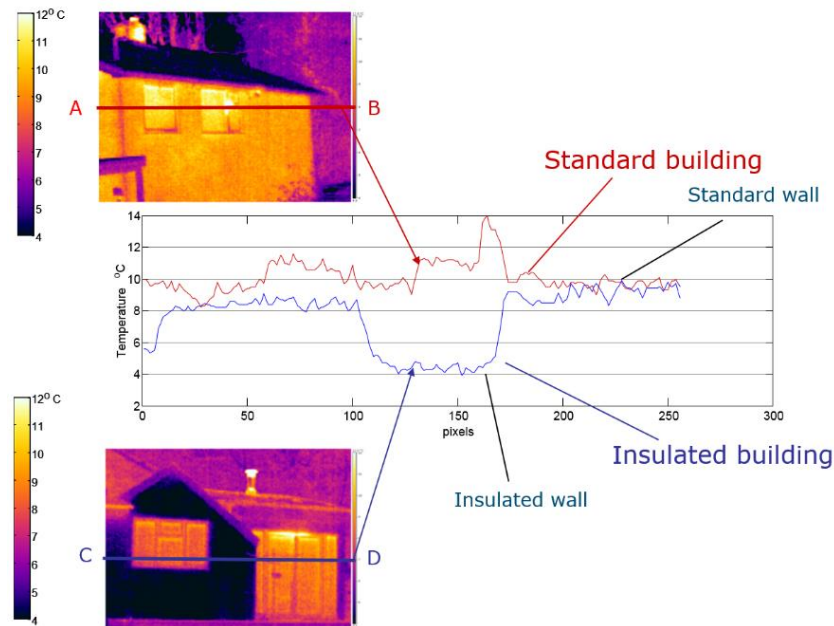

Figure 15: Temperature profiles across the two buildings.

As the surface temperatures of the doors and windows of the insulated building are higher than the ambient temperature, it will be expected that the heat losses in the insulated building occur mainly through doors and windows. In contrast, the temperature profile of line CD indicates that the wall surface temperature of the insulated building remains between 4°C and 6°C and, the double-glazed window section's temperature is between 8°C and 9°C. The typical temperature values of wall and window sections extracted from different infrared images are summarized in Table 1.

Table 1: Typical temperature values of wall and window sections extracted from different infrared images

	Elevation of image	Wall Temperature (°C)	Window Temperature (°C)
Insulated Building	East	5	9
	North east	5	9
	North west	5	9
	South east	5	9
	South	4	9
Uninsulated Building	-	10	11

To further understand the effect of insulation during summer, the internal and external temperatures of the house are recorded from 4th June to 10th June 2011. The internal temperature profiles of the three bedrooms, kitchen, living room and office are shown with the

external temperature profile for the above mentioned seven-day period in Figures 16-a to 16-f respectively.
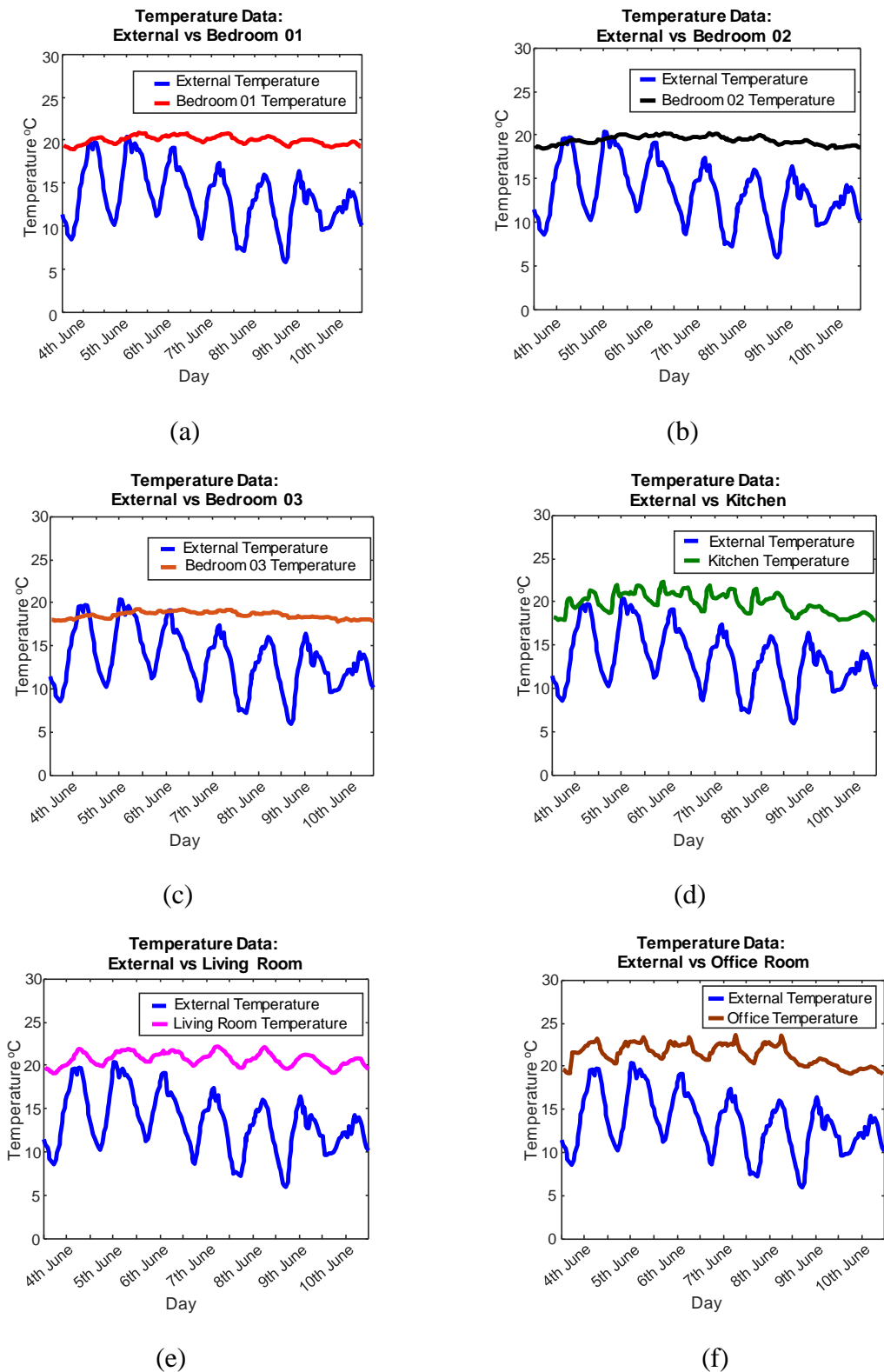

Figure 16: The external and internal temperature profiles of the building from 4th June to 10th June 2011: (a) external temperature vs bedroom 01, (b) external temperature vs bedroom 02, (c) external temperature vs bedroom 03, (d) external temperature vs kitchen, (e) external temperature vs living room, (f) external temperature vs office. (reproduced from seminar presentation of "Greening The Box™ –

Retrofit of Hard to Treat Housing" by John Chilton and Amin Al-Habaibeh at Nottingham Trent University [65].

The maximum temperature, minimum temperature, average temperature and the range of variation in temperature for each case are shown in Table 2. It is found from the table that, in spite of the large variation in external temperature, the internal temperature shows a lower diurnal variation in all rooms. Figures 16-a, b and c show that all three bedrooms have lower variation in temperature than the living room, office and kitchen. This is for three reasons. Firstly, the ground floor rooms are less exposed to solar irradiation and, as a result, the heat gain is lower than the upper floor.

Table 2: The maximum, minimum and average temperatures of external environment, bedroom 01, bedroom 02, bedroom 03, kitchen, living room and office, from 4th to 10th June 2011.

Rooms	Maximum Temperature (ºC)	Minimum Temperature (ºC)	Average Temperature (ºC)	Range of Variation (ºC)
External	20.34	5.88	13.54	14.46
Bedroom 01	20.92	18.87	20.03	2.05
Bedroom 02	20.20	18.38	19.36	1.82
Bedroom 03	19.31	17.76	18.63	1.55
Kitchen	22.27	17.71	19.98	4.56
Living Room	22.11	19.07	20.73	3.04
Office	23.58	19.16	21.56	4.42

Table 2 also reveals that the maximum and minimum temperatures of all three bedrooms are lower than those rooms on the first floor. Secondly, the bedrooms are likely to be occupied during the night only (typically about 8 hours), with sleeping occupants, and therefore the internal heat gain is low. Figures 16-d, e and f show the temperature variation in the kitchen, living room and office respectively. They have higher fluctuation in internal temperature compared to the bedrooms. The highest variation in temperature is found in the kitchen and this is most likely because of cooking activities. The living room and office tend to be mostly occupied during the daytime and evening hours, hence the internal heat gain is higher than those of the bedrooms. A third possible reason is the natural buoyancy of warm air, which means that the first-floor rooms will tend to be warmer than those on the ground floor. In addition, the larger area of windows could also influence the heat gain during daytime. Furthermore, the temperature variation in bedroom 1 and bedroom 2 are slightly higher than that of bedroom 3 as bedroom 1 and bedroom 2 are south facing (Figure 5-c) and hence more exposed to solar irradiation. This could be also a reason for the higher temperature in the upper floor as the three rooms in the upper floor have more exposure to the external environment within the south side (see Figure 5-b). With the large variation in external temperature, the overall variation in internal temperature remains small and this indicates that insulation of the heavy masonry significantly contributes to maintain a steady internal temperature. It is observed in Figures 16-b and 16-c that the internal temperature of bedroom 2 and bedroom 3 remain lower than the external temperature in the afternoons of 4th and 5th June. Hence, it can be said that a well-designed insulation in some cases could prevent houses from being extra warm in summer months as well. Using the maximum values of wall temperature from Table 1 in equation (4), the estimated heat losses through the uninsulated wall is about 45.62 W/m² and the estimated heat losses through the insulated wall is about 7.61 W/m². The data in Table 1 shows that at 4ºC ambient temperature, the insulated wall surface temperature is 5ºC and the

uninsulated wall surface temperature is at 10°C. Assuming the room temperature to be at 20°C for both buildings throughout the year, the external wall temperature of both walls will be similar to the ambient temperature when the ambient temperature rises to 20°C in summer. It is assumed in the analysis that double-glazed windows have the same performance for both buildings and there will be no air-conditioning.
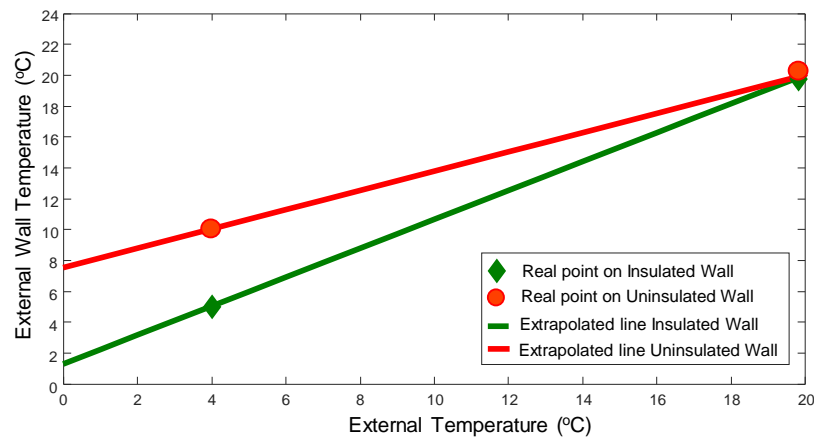

Figure 17: The relationship between the external ambient temperature and external wall temperature.

The walls' temperature for both buildings relative to different ambient temperatures can be obtained by using interpolation within this range as shown in Figure 17. The outdoor temperature varies day to day as well as at different times during the same day. To even out this variation, the hourly temperature of each day for a whole month is averaged and that monthly average temperature is used in this study. Considering the average temperature for each month during that year extracted from historical temperature data of that locality, and estimating wall temperature for both buildings from Figure 17, the net difference in heat losses between the two buildings are estimated in Table 3 using equation (5).

Table 3: The estimated heat loss through insulated and uninsulated walls in different months of a typical year.

Month	Average External Temperature (°C)	External Wall Temperature (°C)		Heat Loss (kWh/m^2) for whole month		Difference in Heat Loss (kWh/m^2) for the month
		Insulated Building	Uninsulated Building	Insulated Building	Uninsulated Building	
Jan	4.50	5.47	10.31	5.49	32.91	27.42
Feb	7.00	7.81	11.88	4.16	24.93	20.77
Mar	7.40	8.19	12.13	4.46	26.76	22.30
Apr	12.70	13.16	15.44	2.50	15.00	12.50
May	13.20	13.63	15.75	2.41	14.44	12.03
Jun	14.90	15.22	16.81	1.75	10.48	8.73
Jul	16.00	16.25	17.50	1.42	8.49	7.07
Aug	16.20	16.44	17.63	1.34	8.07	6.73
Sep	15.60	15.86	17.25	1.51	9.04	7.53
Oct	13.00	13.48	15.63	2.48	14.87	12.39

|						
Nov	10.50	11.09	14.06	3.25	19.52	16.27
Dec	6.80	7.63	11.75	4.67	28.03	23.36
Total				**35.44**	**212.54**	**177.10**

As the total heat loss through a building's wall depends on the size and shape of that building, heat loss per square meter has been considered to compare between insulated and uninsulated walls. Table 3 shows the heat loss through walls of the insulated and uninsulated building for each month as well as the difference in heat losses between the two buildings. According to Table 3, the energy savings due to retrofitting for 1 m^2 of wall area is 177.10 kWh. Therefore, the energy savings for a typical three bedroom house with 120 m^2 of wall area exposed to external environment will be 177.10 $kWh/m^2 \times 120\,m^2 = 21,252\,kWh$. This implies around £2741.51 per annum of savings in electricity bills at a rate of 12.90 pence/kWh excluding VAT or, around £612.06 per annum of savings in gas bills at a rate of 2.88 pence/kWh excluding VAT for the household during winter[66].

*4.2* **ANN prediction of heat losses and energy savings**

The predicted heat losses for the years 2015, 2016 and 2017 by the ANN, that has been trained with the calculated heat losses of years 2010 to 2014, are shown in Figure 18. Figure 18-a, c and e represent the calculated and predicted output of the ANN for the heat loss profiles through the insulated wall for the years 2015, 2016 and 2017 respectively. Figure 18-b, d and f represent similar profiles of heat losses through the uninsulated wall for the above-mentioned years. It has been found from Figure 18-a and b that the ANN predicted the heat losses at higher levels than the calculated heat losses in December 2015 for both types of wall. The local historical temperature map, as in Figure 19, shows that 2015 has experienced a warmer December than the previous 5 years; hence, the calculated heat losses in December 2015 are less than that of the past 5 years. As ANN learns the features of the training data, it predicts higher heat losses than the calculated values based on the past 5 years of training data. However, 2016 and 2017 experienced cooler December than 2015, and the ANN predicted heat losses of those periods at a closer level. Now, the ANN is trained with heat losses data of years 2010 to 2015 and the prediction is made for years 2016 and 2017 for both types of walls, as shown in Figure 20. The predicted profiles have shown a significant drop in heat losses in December 2016. However, with the inclusion of heat losses data from year 2016 for training, the predicted heat losses for December become very close to the calculated heat losses, see Figure 21. It is also noticed that in all profiles of Figure 18 that there is a small peak in the profiles of ANN predicted heat losses in August. According to Figure 19, the average temperature in August in 2015 and 2016 is found higher than the average of the previous 5 years. As a result, the calculated heat losses in year 2015 and 2016 are less than those of the previous 5 years during August. This is not reflected in the ANN prediction of heat losses because ANN depends on the data pattern of the training data set. The temperature in August of 2017 is found to be near the average temperature in August of the years 2010 to 2014; and hence, the ANN predicted similar heat losses in August when compared to the calculated values (see Figure 18-e and f). The inclusion of further heat losses data from years 2015 and 2016 for training has altered the situation, where the predicted heat losses are closer to the calculated heat losses for the year 2016 and less than those for the year 2017 (Figure 20 and 21). There are further aberrant predictions found in September 2017 as in Figure 21. This is due to adding the heat losses data from the year 2016 in the training data set. The month of September in 2016 is found to be the warmest among all Septembers from year 2010 to 2016. Hence, the calculated heat losses for September 2016 is the least among all other Septembers in that period. The ANN replicates this feature in the prediction of heat losses for 2017's September; and hence, elicit noticeable differences.
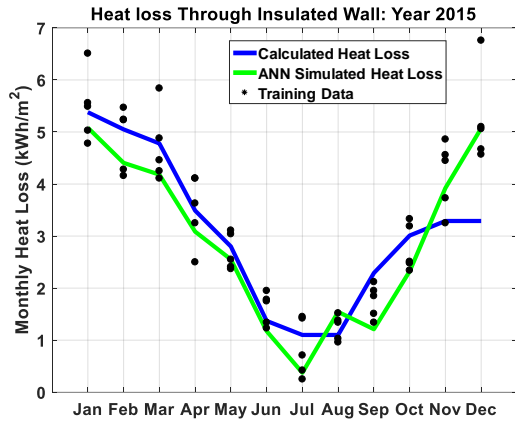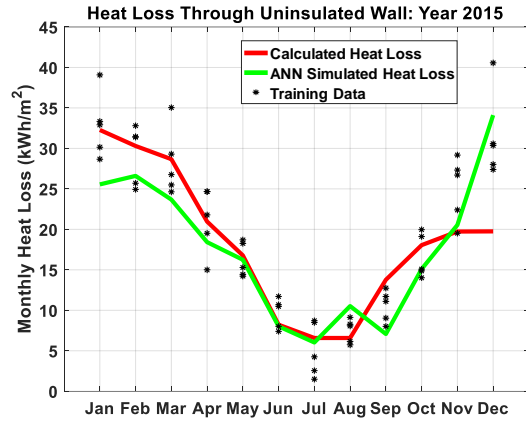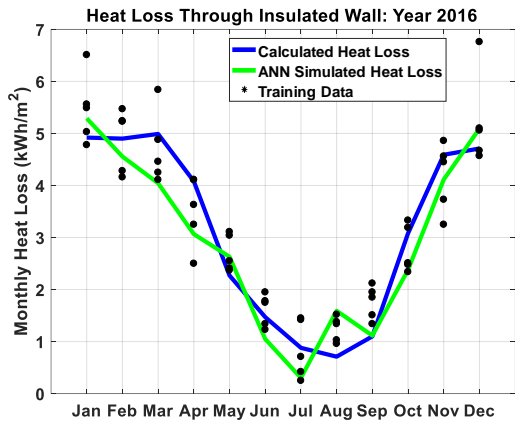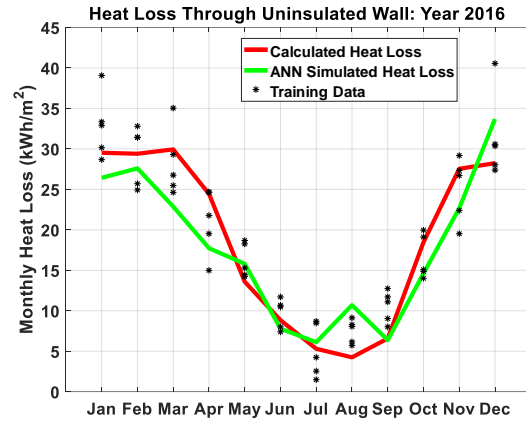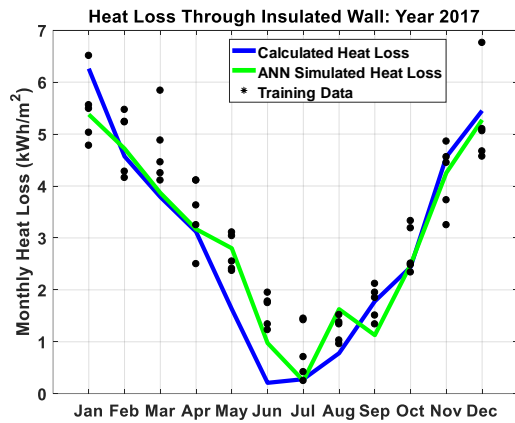
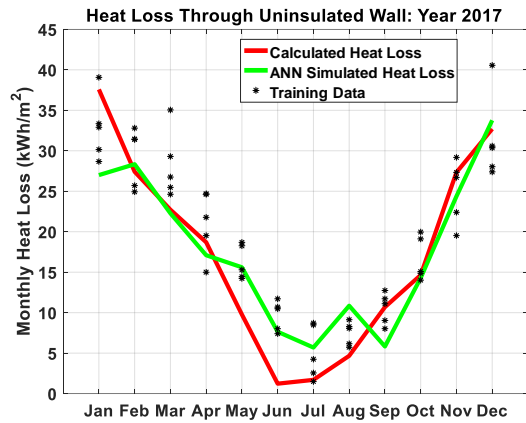Figure 18: The comparison between calculated heat loss and ANN simulated heat loss through the insulated and uninsulated wall for years 2015, 2016 and 2017.
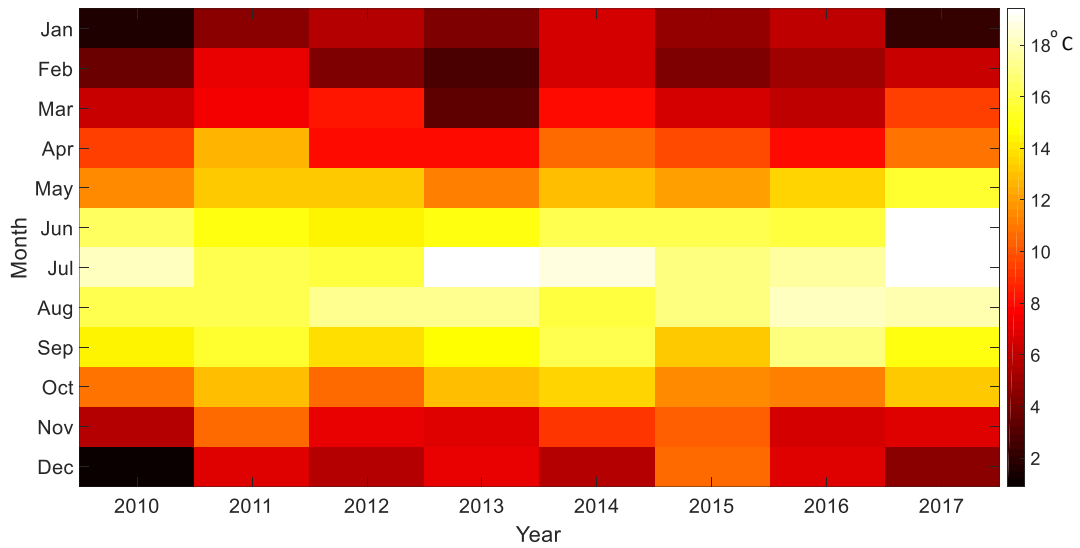
Figure19: The historical monthly average temperature map from year 2010 to 2017 of that locality.
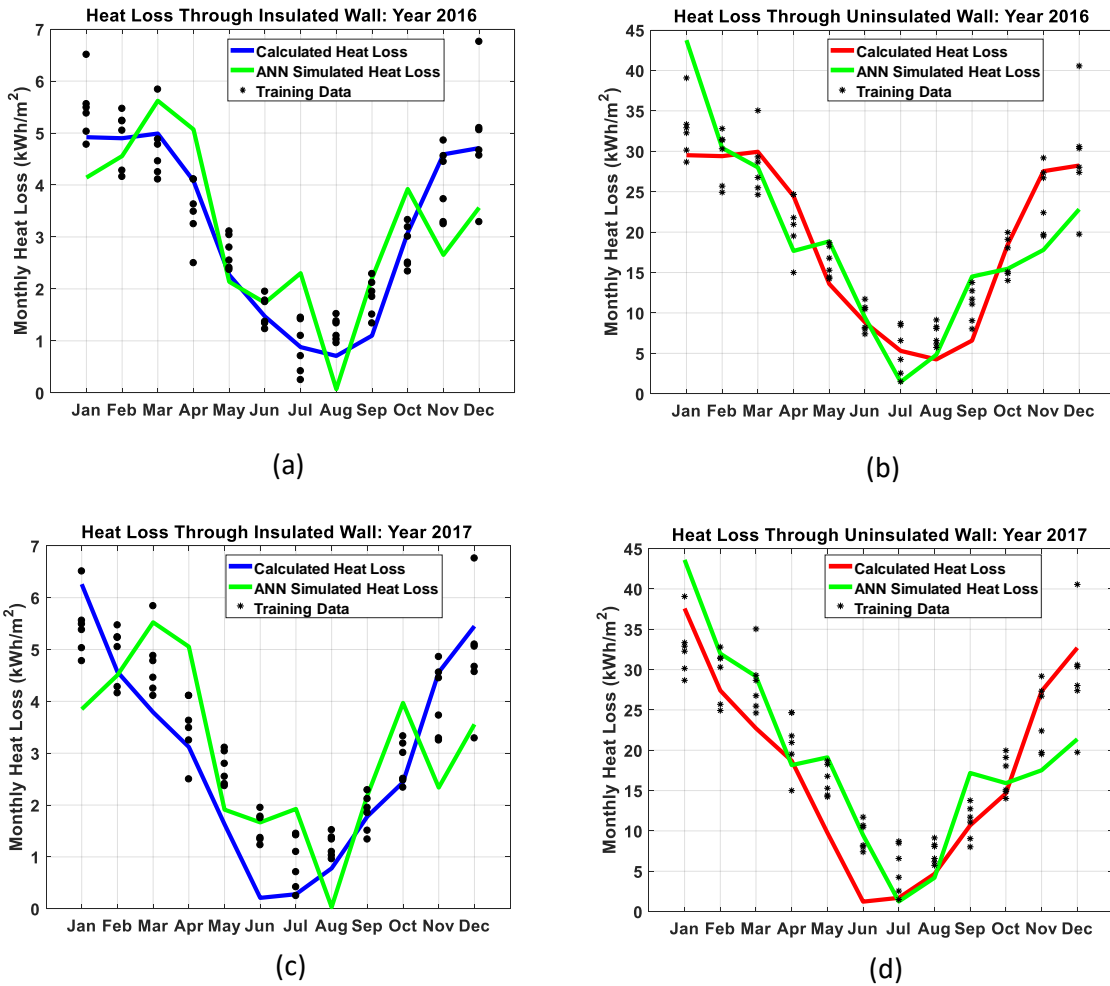

(a)

(b)

(c)

(d)

Figure 20: The comparison between the calculated heat loss and ANN predicted heat loss through the insulated and uninsulated wall for years 2016 and 2017.
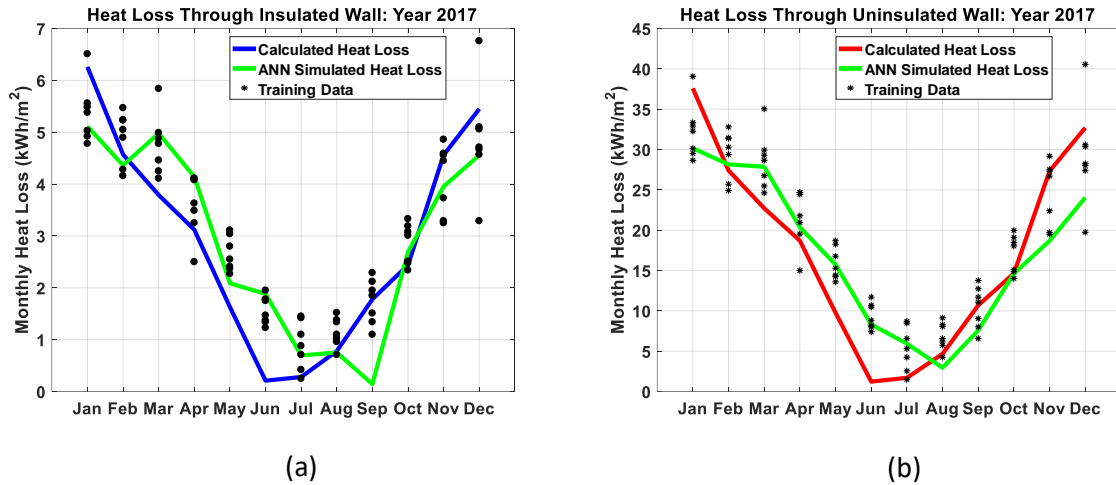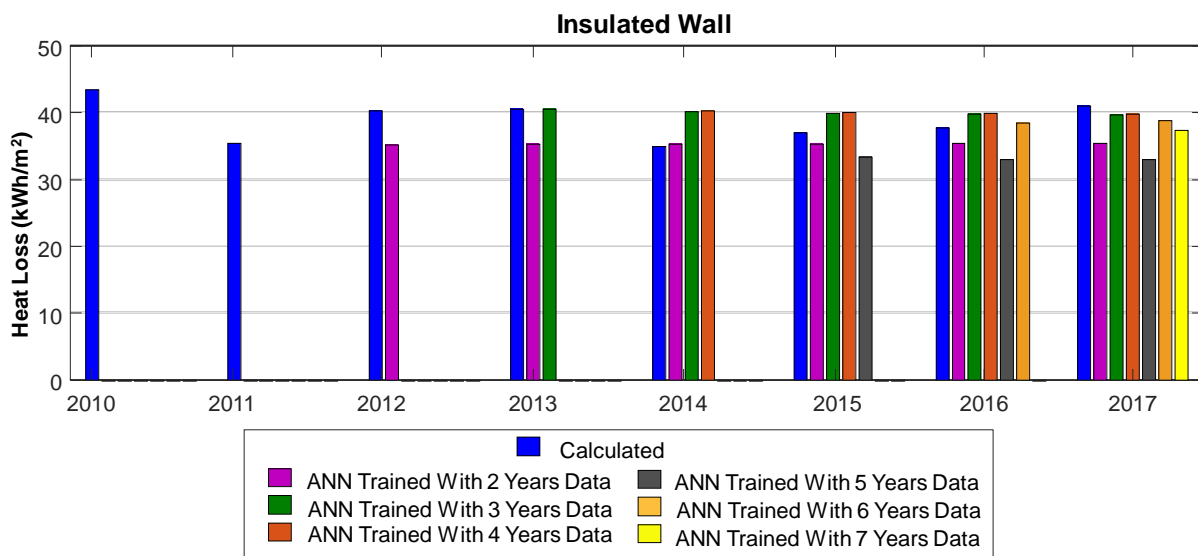
Figure 21: The comparison between the calculated heat loss and ANN simulated heat loss through the insulated and uninsulated wall for the year 2017.

From the analysis of above figures, it has been found that ANN predictions of heat losses for both insulated and uninsulated walls show good agreement with the calculated heat losses in most of the cases, though there are some nonconformities in some predictions. These nonconformities arise due to the variation in the calculated heat losses data, which is not exactly featured by the training data sets. Furthermore, the position of predicted curves in Figure 18, 20 and 21 versus the training data confirms that there is no overfitting in the prediction process.

Figure 22 represents the comparison between the calculated yearly heat losses and ANN predictions of yearly heat losses with different training data sets for the insulated and uninsulated walls. As data from 2010 and 2011 are used for training, no predictions are possible for those two years. The highest number of predictions are made for 2017 as this is the only year that is not included in the training process. It is noted in Figure 22 that the ANN predicted heat losses are slightly higher than the calculated ones in 14 out of 21 cases for each wall type, which signifies the tendency of ANN to overestimate the heat losses in this case. However, one consistency that is also noticed from both figures that if the ANN overestimates the heat loss for the insulated wall, it also overestimates the figure for the uninsulated wall; and similarly for the underestimation process. This is also noted in Figure 23, which shows the percentage error (e_p) in the prediction made by the ANN with different training data sets. The direction of the error is the same in each case for both walls. Figure 23 also reveals that the range of error for the insulated wall is -13% to +15%, and for the uninsulated wall is -14% to +17.5%. The uninsulated wall has higher error range than the insulated wall, as the heat losses for the uninsulated wall are much higher. Considering the highest limit of error range, it can be said that the ANN can predict heat losses through building's wall with at least 82.5% accuracy regardless of the wall type and training data size. However, the pattern of percentage error is not conclusive enough to identify the type of wall. Figure 24-a represents the absolute values of percentage error ($|e_p|$) in each year's predictions for the insulated and uninsulated walls and Figure 24-b represents the average $|e_p|$ per year of the predictions made by the ANN with different training data sets. From these two figures, it is observed that there is no correlation between the prediction error and the size of the training data set. For instance, if we consider year 2017 in Figure 24-a, the percentage error of the ANN trained with three years of data is higher than that of the ANN when trained with two years of data. However, the percentage

error of the ANN trained with five years of data is less than that of the ANN when trained with four years of data. The percentage error again rises when the ANN is trained with six years of data followed by a drop when it is trained with seven years of data. Figure 24-b also conveys similar information as the absolute percentage error per year is found higher for the ANN when trained with three years of data than for the ANN trained with two years of data. On the other hand, the absolute percentage error per year becomes less for the ANN trained with five years of data than for the ANN trained with four years of data. Again, the percentage error per year rises when the ANN is trained with six years of data. It is also noticed that the absolute percentage error for the uninsulated wall is higher than that of the insulated wall in majority of cases.

(a)
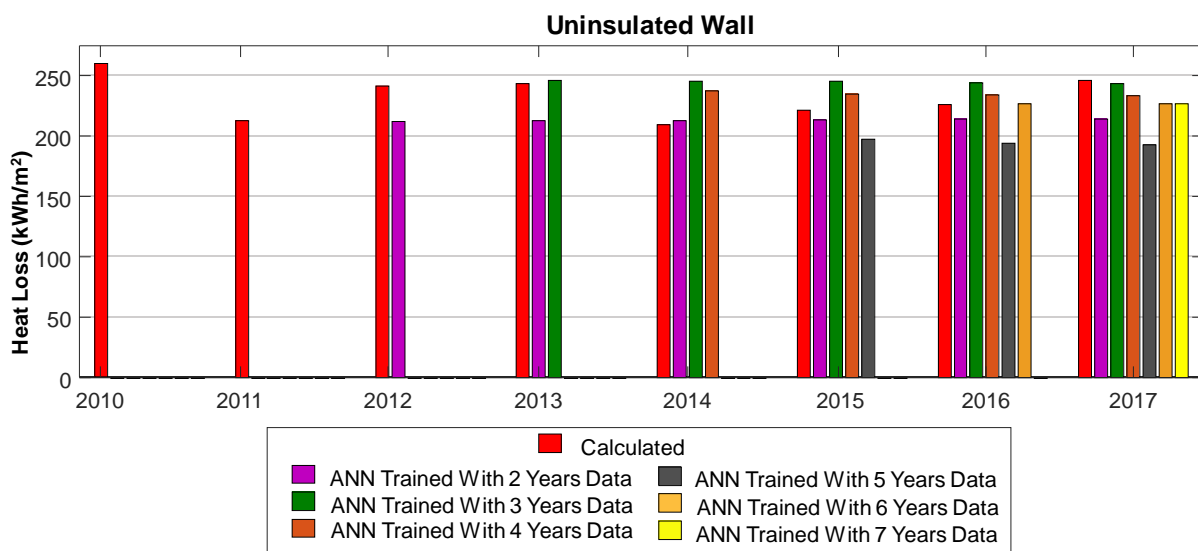
(b)

Figure 22: The comparison between the calculated yearly heat losses and ANN predictions of yearly heat losses with different training data set for (a) insulated wall; and (b) uninsulated wall.
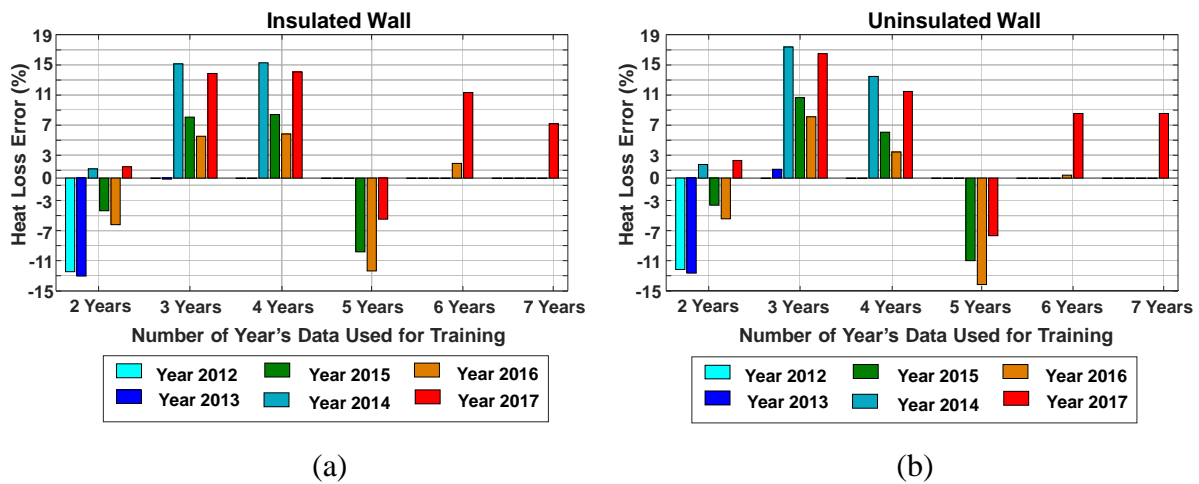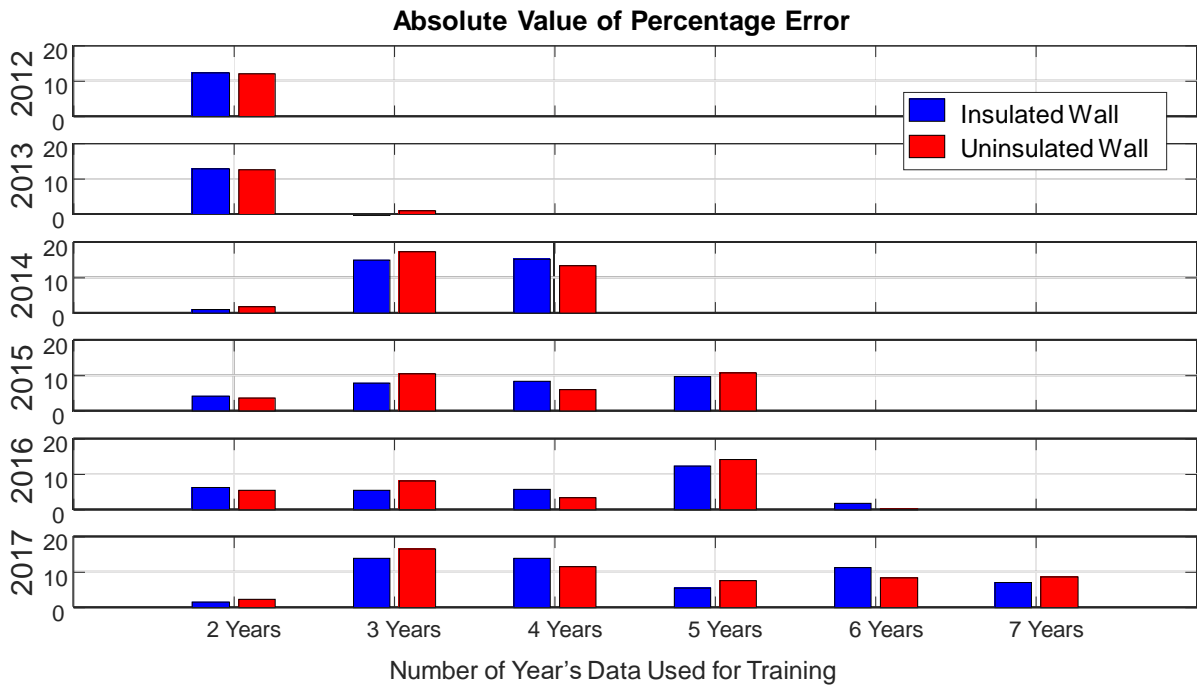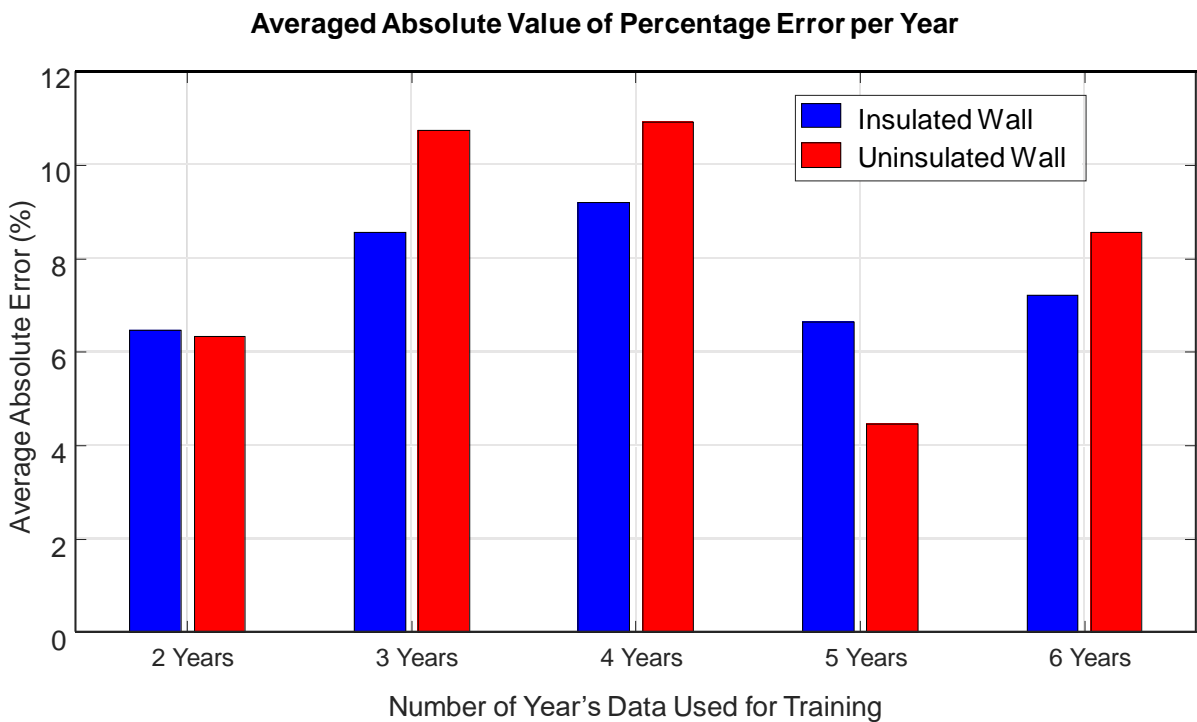
Figure 23: The percentage error in the ANN predicted yearly heat losses with different data set for (a) insulated wall; and (b) uninsulated wall.

Due to global warming, ambient temperature prediction tends to be less accurate, and this phenomenon influences the prediction of the energy loss because heat losses of a building have a direct relationship with ambient temperature. Considering the change in ambient temperature by $\pm 1^{\circ}$C, the percentage error in the ANN prediction is summarised in Figure 25-a and b for the insulated and uninsulated walls respectively. If the environmental temperature decreases or increases by 1°C, then the actual heat loss will be more or less than that of normal situation respectively. Hence, it is revealed from the above figures that the percentage error in prediction of the ANN ranges between -20.68% and +29.68% for the insulated wall and between -20.48% and +33.32% for the uninsulated wall. Again, the percentage error is higher for the uninsulated wall than that of the insulated wall because of the higher level of heat losses. Considering the effect of global warming, the minimum accuracy of the ANN prediction will drop from 82.5% to 66.68% in case of $\pm 1^{\circ}$C change in ambient temperature. It is worth mentioning that monitoring a building for a year or more before and after retrofitting to estimate the benefits could be time consuming and expensive. Particularly with the variation in weather conditions and people's behaviour, as we have seen mathematically. Therefore, in this paper the proposed approach has utilised a simplified and a rapid method to evaluate the benefits using key parameters, infrared thermography and deep learning neural networks. This should provide a tool to encourage the owners of non-insulated buildings to assess the benefits of insulation to improve thermal insulation.
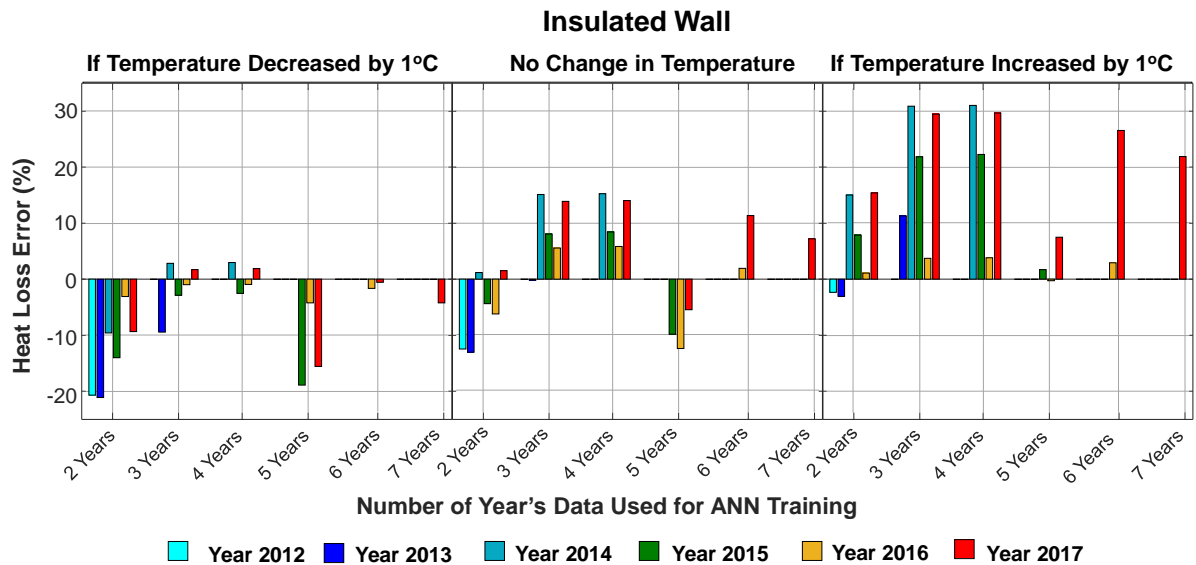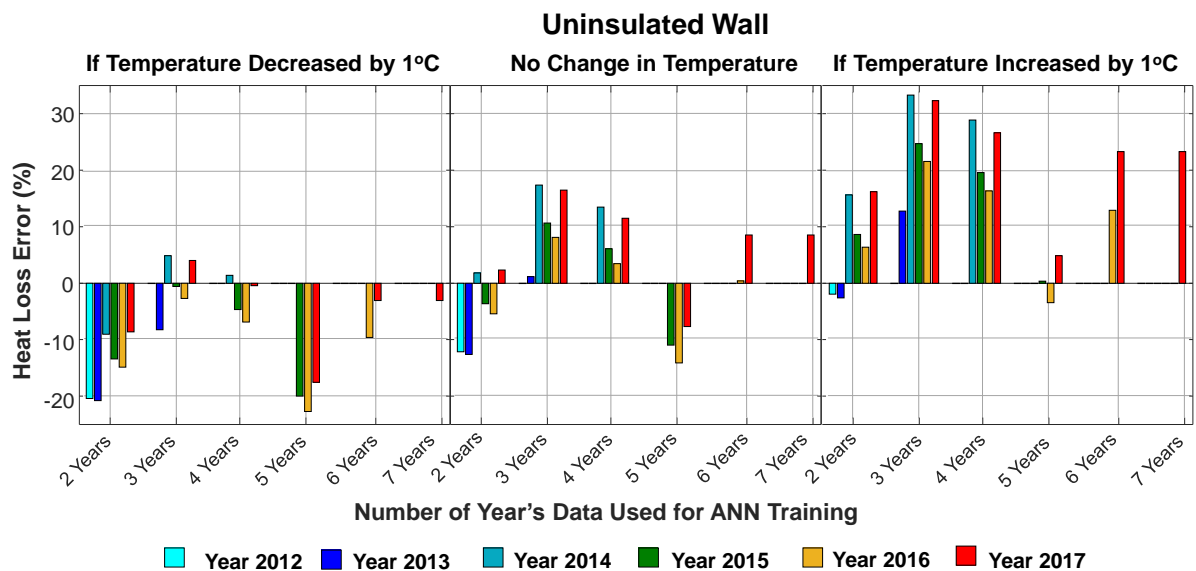
(a)

(b)

Figure 24: The percentage error in the ANN predicted yearly heat losses through insulated and uninsulated wall, (a) absolute values of percentage error; and (b) averaged absolute value of percentage error per year.

Insulated Wall

(a)

Uninsulated Wall

(b)

Figure 25: The percentage error in the prediction of the ANN if the temperature is changed by ±1°C , (a) insulated wall; and (b) uninsulated wall.

5. Limitations and assumptions of the simulation technique

Buildings go through complex environmental and weather conditions as well as significant variation in occupants' behaviour. Given such complexity, it will be difficult to provide exact figures about energy savings regardless of the efforts used in the simulation and real data analysis. Therefore, the authors acknowledge such limitations and have assumed some average values of the environmental parameters to estimate energy savings. For example, wind speed and direction vary greatly over time; and hence an average value estimated from previous studies have been used. The effect of thermal bridges is ignored, as normally the area of any thermal bridging will be small when compared to the area of whole wall to influence the overall

heat loss. Hence the effect of thermal bridges is not considered during this comparison process. An assumption is made that heating will be switched on when the ambient temperature below 20°C. This might have its own limitations since during summer, the temperature falls below 20°C at night but the heat losses in most cases are offset by daytime solar gain. Therefore, in most cases no space heating is used in the UK during that period of the year. We have assumed heating will be on at any time when the ambient temperature is below 20°C for the payback period calculations. As discussed in this paper, mathematically the number of years should be infinite (i.e. life-time monitoring to achieve accurate comparison for the effect of insulation and the payback period).

6. Conclusion

To meet the goal of the UK Government's Climate Change Act (2008), reduction in energy consumption should have priority over the reduction in carbon emission at the source of energy production [67]. Heating and air-conditioning is responsible for the major part of energy consumption in buildings. Insulation can play a significant role in improving thermal performance of buildings by restricting heat losses and reducing energy consumption for heating and air-conditioning. The key conclusions of this work are as follows:

- As demonstrated by the estimated monthly heat losses given in Table 3, there is a potential for annual energy savings of about 80% for the retrofitted and externally insulated building when compared to an equivalent uninsulated building.
- Infrared thermography is a very effective tool in evaluating buildings' thermal performance. The results of the case study presented in this paper show a very good agreement with that.
- It is demonstrated from the weeklong monitoring of indoor and outdoor temperatures that insulation could aid in maintaining a steady indoor temperature during summer as well as during the heating season.
- The novel use of ANN combined with infrared thermography data is found to be capable of predicting future heat losses with over 82% accuracy regardless of wall type and training data size.
- The heat loss predictions can be used to estimate future energy savings due retrofitting; and consequently, rationalise the investment on retrofitting in terms of savings on energy bills. Hence the suggested novel approach provides a tool for rapid analysis of energy savings for communities.
- The use of infrared thermography combined with ANN can support architects and energy consultants to rapidly evaluate the effectiveness of wall insulation for a particular locality without using expensive energy simulation software.
- In order to accurately estimate the energy savings from insulation, this paper has proved mathematically that a life-long monitoring will be needed.

Simplicity and practicality of this novel approach to characterise buildings' energy performance is the key objective of this paper. Real buildings in real world are affected by variable wind speed, variable sun position and people's behaviour. Hence, monitoring the same building over several years will most likely to lead to different results in any case. Using a simplified model with some given assumptions will provide sufficient information and data estimation about the potential performance of a building and enable modelling the main factors that influence its thermal behaviour. In this way, it will produce a reasonable comparison in relatively a short period of time by focusing on the insulation factor.

Acknowledgment

References:

[1]   U.S. Energy Information Administration, "International Energy Outlook 2017," 2017. Accessed: Nov. 28, 2017. [Online]. Available: https://www.eia.gov/outlooks/ieo/pdf/0484(2017).pdf.

[2]   United Nations Framework Convention on Climate Change, "ADOPTION OF THE PARIS AGREEMENT - Paris Agreement text English." United Nations, Paris , pp. 1–27, 2015, Accessed: Jul. 19, 2017. [Online]. Available: https://unfccc.int/files/essential_background/convention/application/pdf/english_paris_agreement.pdf.

[3]   *Climate Change Act*. London: The Parliament of the United Kingdom, 2008, pp. 1–103.

[4]   Committee on Climate Change, "UK Climate Action Following the Paris Agreement," London, 2016. Accessed: Jul. 19, 2017. [Online]. Available: https://www.theccc.org.uk/wp-content/uploads/2016/10/UK-climate-action-following-the-Paris-Agreement-Committee-on-Climate-Change-October-2016.pdf.

[5]   UK Green Building Council, "Delivering Low Carbon Infrastructure." pp. 1–32, 2017, Accessed: Jul. 19, 2017. [Online]. Available: http://www.ukgbc.org/sites/default/files/Delivering Low Carbon Infrastructure.pdf.

[6]   U.S. Energy Information Administration, "International Energy Outlook 2016," 2016. doi: www.eia.gov/forecasts/ieo/pdf/0484(2016).pdf.

[7]   Department for Business Energy & Industrial Strategy, "Digest of United Kingdom Energy Statistics 2016." pp. 1–266, 2016, [Online]. Available: https://www.gov.uk/government/uploads/system/uploads/attachment_data/file/577712/DUKES_2016_FINAL.pdf.

[8]   Department for Business Energy & Industrial Strategy, "ENERGY CONSUMPTION IN THE UK," London, 2017. Accessed: Nov. 28, 2017. [Online]. Available: https://www.gov.uk/government/uploads/system/uploads/attachment_data/file/633503/ECUK_2017.pdf.

[9]   A. Haslett, "HOUSING RETROFITS – A NEW START," 2016. [Online]. Available: https://d2umxnkyjne36n.cloudfront.net/insightReports/Housing-Retrofits-A-New-Start.pdf?mtime=20161111100257.

[10]   The Construction 2025, "Industrial Strategy: government and industry in partnership," 2013. Accessed: Jul. 20, 2017. [Online]. Available: https://www.gov.uk/government/uploads/system/uploads/attachment_data/file/210099/bis-13-955-construction-2025-industrial-strategy.pdf.

[11]   J. Adamczyk and R. Dylewski, "The impact of thermal insulation investments on sustainability in the construction sector," *Renew. Sustain. Energy Rev.*, vol. 80, no. December 2016, pp. 421–429, Dec. 2017, doi: 10.1016/j.rser.2017.05.173.

[12]   L. Aditya *et al.*, "A review on insulation materials for energy conservation in buildings," *Renew. Sustain. Energy Rev.*, vol. 73, no. February, pp. 1352–1365, Jun. 2017, doi: 10.1016/j.rser.2017.02.034.

[13] J. Kim and J. W. Moon, "Impact of Insulation on Building Energy Consumption," *Build. Simul. 2009*, pp. 674–680, 2009, [Online]. Available: http://citeseerx.ist.psu.edu/viewdoc/summary?doi=10.1.1.172.4791.

[14] A. Byrne, G. Byrne, G. O'Donnell, and A. Robinson, "Case studies of cavity and external wall insulation retrofitted under the Irish Home Energy Saving Scheme: Technical analysis and occupant perspectives," *Energy Build.*, vol. 130, pp. 420–433, Oct. 2016, doi: 10.1016/j.enbuild.2016.08.027.

[15] J. Lee, J. Kim, D. Song, J. Kim, and C. Jang, "Impact of external insulation and internal thermal density upon energy consumption of buildings in a temperate climate with four distinct seasons," *Renew. Sustain. Energy Rev.*, vol. 75, no. November 2016, pp. 1081–1088, Aug. 2017, doi: 10.1016/j.rser.2016.11.087.

[16] T. Berger *et al.*, "Impacts of external insulation and reduced internal heat loads upon energy demand of offices in the context of climate change in Vienna, Austria," *J. Build. Eng.*, vol. 5, pp. 86–95, Mar. 2016, doi: 10.1016/j.jobe.2015.11.005.

[17] Z. Fang, N. Li, B. Li, G. Luo, and Y. Huang, "The effect of building envelope insulation on cooling energy consumption in summer," *Energy Build.*, vol. 77, pp. 197–205, Jul. 2014, doi: 10.1016/j.enbuild.2014.03.030.

[18] L. Derradji, K. Imessad, M. Amara, and F. Boudali Errebai, "A study on residential energy requirement and the effect of the glazing on the optimum insulation thickness," *Appl. Therm. Eng.*, vol. 112, pp. 975–985, 2017, doi: 10.1016/j.applthermaleng.2016.10.116.

[19] E. Kossecka and J. Kosny, "Influence of insulation configuration on heating and cooling loads in a continuously used building," *Energy Build.*, vol. 34, no. 4, pp. 321–331, May 2002, doi: 10.1016/S0378-7788(01)00121-9.

[20] D. I. Kolaitis, E. Malliotakis, D. A. Kontogeorgos, I. Mandilaras, D. I. Katsourinis, and M. A. Founti, "Comparative assessment of internal and external thermal insulation systems for energy efficient retrofitting of residential buildings," *Energy Build.*, vol. 64, pp. 123–131, Sep. 2013, doi: 10.1016/j.enbuild.2013.04.004.

[21] D. Wang, W. Yu, X. Zhao, W. Dai, and Y. Ruan, "The influence of thermal insulation position in building exterior walls on indoor thermal comfort and energy consumption of residential buildings in Chongqing," *IOP Conf. Ser. Earth Environ. Sci.*, vol. 40, p. 012081, Aug. 2016, doi: 10.1088/1755-1315/40/1/012081.

[22] A. Reilly and O. Kinnane, "The impact of thermal mass on building energy consumption," *Appl. Energy*, vol. 198, pp. 108–121, Jul. 2017, doi: 10.1016/j.apenergy.2017.04.024.

[23] L. Zhang, J. Zhang, F. Wang, and Y. Wang, "Effects of wall masonry layer's thermophysical properties and insulation position on time lag and decrement factor," *Indoor Built Environ.*, vol. 25, no. 2, pp. 371–377, Apr. 2016, doi: 10.1177/1420326X14551615.

[24] L. Long and H. Ye, "The roles of thermal insulation and heat storage in the energy performance of the wall materials: a simulation study," *Sci. Rep.*, vol. 6, no. 1, p. 24181, Jul. 2016, doi: 10.1038/srep24181.

[25] K. Menyhart and M. Krarti, "Potential energy savings from deployment of Dynamic

Insulation Materials for US residential buildings," *Build. Environ.*, vol. 114, pp. 203–218, Mar. 2017, doi: 10.1016/j.buildenv.2016.12.009.

[26]   A. Staszczuk, M. Wojciech, and T. Kuczyński, "The effect of floor insulation on indoor air temperature and energy consumption of residential buildings in moderate climates," *Energy*, vol. 138, pp. 139–146, Nov. 2017, doi: 10.1016/j.energy.2017.07.060.

[27]   E. Lucchi, "Applications of the infrared thermography in the energy audit of buildings: A review," *Renew. Sustain. Energy Rev.*, vol. 82, pp. 3077–3090, Feb. 2018, doi: 10.1016/J.RSER.2017.10.031.

[28]   Flir System, "ThermaCAM™ E25 User's manual." 2006, Accessed: Dec. 18, 2018. [Online]. Available: http://sti-monge.fr/maintenancesystemes/wp-content/uploads/2013/06/FLIR-E25-Manual.pdf.

[29]   CIBSE, "CIBSE Guide A: Environment Design." Elsevier, pp. 1–323, 2006, [Online]. Available: hhttp://www.cibse.org/getattachment/Knowledge/CIBSE-Guide/CIBSE-Guide-A-Environmental-Design-NEW-2015/Guide-A-presentation.pdf.aspx.

[30]   G. I. C. Hartig, K.W., Larson, S.L. and Lingle, P.J., "Low-E glass coating system and insulating glass units made therefrom," May 07, 1996.

[31]   A. Hoyano, K. Asano, and T. Kanamaru, "Analysis of the sensible heat flux from the exterior surface of buildings using time sequential thermography," *Atmos. Environ.*, vol. 33, no. 24–25, pp. 3941–3951, Oct. 1999, doi: 10.1016/S1352-2310(99)00136-3.

[32]   R. Usamentiaga *et al.*, "Infrared Thermography for Temperature Measurement and Non-Destructive Testing," *Sensors*, vol. 14, no. 7, pp. 12305–12348, Jul. 2014, doi: 10.3390/s140712305.

[33]   A. Kylili, P. A. Fokaides, P. Christou, and S. A. Kalogirou, "Infrared thermography (IRT) applications for building diagnostics: A review," *Appl. Energy*, vol. 134, pp. 531–549, Dec. 2014, doi: 10.1016/j.apenergy.2014.08.005.

[34]   I. Danielski and M. Fröling, "Diagnosis of Buildings' Thermal Performance - A Quantitative Method Using Thermography Under Non-steady State Heat Flow," *Energy Procedia*, vol. 83, no. 83, pp. 320–329, Dec. 2015, doi: 10.1016/j.egypro.2015.12.186.

[35]   B. M. Marino, N. Muñoz, and L. P. Thomas, "Estimation of the surface thermal resistances and heat loss by conduction using thermography," *Appl. Therm. Eng.*, vol. 114, pp. 1213–1221, 2017, doi: 10.1016/j.applthermaleng.2016.12.033.

[36]   F. Asdrubali, G. Baldinelli, and F. Bianchi, "A quantitative methodology to evaluate thermal bridges in buildings," *Appl. Energy*, vol. 97, pp. 365–373, Sep. 2012, doi: 10.1016/J.APENERGY.2011.12.054.

[37]   R. Albatici, A. M. Tonelli, and M. Chiogna, "A comprehensive experimental approach for the validation of quantitative infrared thermography in the evaluation of building thermal transmittance," *Appl. Energy*, vol. 141, pp. 218–228, Mar. 2015, doi: 10.1016/j.apenergy.2014.12.035.

[38]   A. Al-Habaibeh and F. L. Siena, "The Application of Infrared Thermography for The Evaluation of Insulation and Energy Performance of Buildings," in *4th. JIIRCRAC 2012, Amman-Jordan,* 2012.

[39] A. Al-Habaibeh, B. Medjdoub, and A. Pidduck, "Investigating The Influence of Door Design on The Energy Consumption of Buildings Using Infrared Thermography," in *4th. JIIRCRAC 2012, Amman-Jordan, Sept. 10th – 12th 2012*, 2012.

[40] D. Bienvenido-Huertas, J. Bermúdez, J. J. Moyano, and D. Marín, "Influence of ICHTC correlations on the thermal characterization of façades using the quantitative internal infrared thermography method," *Build. Environ.*, vol. 149, pp. 512–525, Feb. 2019, doi: 10.1016/j.buildenv.2018.12.056.

[41] B. Xie, C. Li, B. Zhang, L. Yang, G. Xiao, and J. Chen, "Evaluation of stearic acid/coconut shell charcoal composite phase change thermal energy storage materials for tankless solar water heater," *Energy Built Environ.*, Oct. 2019, doi: 10.1016/j.enbenv.2019.08.003.

[42] Z. Wang and R. S. Srinivasan, "A review of artificial intelligence based building energy use prediction: Contrasting the capabilities of single and ensemble prediction models," *Renew. Sustain. Energy Rev.*, vol. 75, pp. 796–808, Aug. 2017, doi: 10.1016/J.RSER.2016.10.079.

[43] Y. Zhang, Z. O'Neill, B. Dong, and G. Augenbroe, "Comparisons of inverse modeling approaches for predicting building energy performance," *Build. Environ.*, vol. 86, pp. 177–190, Apr. 2015, doi: 10.1016/J.BUILDENV.2014.12.023.

[44] B. B. Ekici and U. T. Aksoy, "Prediction of building energy consumption by using artificial neural networks," *Adv. Eng. Softw.*, vol. 40, no. 5, pp. 356–362, May 2009, doi: 10.1016/J.ADVENGSOFT.2008.05.003.

[45] R. Yokoyama, T. Wakui, and R. Satake, "Prediction of energy demands using neural network with model identification by global optimization," *Energy Convers. Manag.*, vol. 50, no. 2, pp. 319–327, Feb. 2009, doi: 10.1016/J.ENCONMAN.2008.09.017.

[46] R. Ž. Jovanović, A. A. Sretenović, and B. D. Živković, "Ensemble of various neural networks for prediction of heating energy consumption," *Energy Build.*, vol. 94, pp. 189–199, May 2015, doi: 10.1016/J.ENBUILD.2015.02.052.

[47] A. E. Ben-Nakhi and M. A. Mahmoud, "Cooling load prediction for buildings using general regression neural networks," *Energy Convers. Manag.*, vol. 45, no. 13–14, pp. 2127–2141, Aug. 2004, doi: 10.1016/J.ENCONMAN.2003.10.009.

[48] A. H. Neto and F. A. S. Fiorelli, "Comparison between detailed model simulation and artificial neural network for forecasting building energy consumption," *Energy Build.*, vol. 40, no. 12, pp. 2169–2176, Jan. 2008, doi: 10.1016/J.ENBUILD.2008.06.013.

[49] F. Martellotta, U. Ayr, P. Stefanizzi, A. Sacchetti, and G. Riganti, "On the use of artificial neural networks to model household energy consumptions," *Energy Procedia*, vol. 126, pp. 250–257, Sep. 2017, doi: 10.1016/j.egypro.2017.08.149.

[50] L. Wang, E. W. M. Lee, and R. K. K. Yuen, "Novel dynamic forecasting model for building cooling loads combining an artificial neural network and an ensemble approach," *Appl. Energy*, vol. 228, pp. 1740–1753, Oct. 2018, doi: 10.1016/J.APENERGY.2018.07.085.

[51] S. Naji *et al.*, "Application of adaptive neuro-fuzzy methodology for estimating building energy consumption," *Renew. Sustain. Energy Rev.*, vol. 53, pp. 1520–1528, Jan. 2016, doi: 10.1016/J.RSER.2015.09.062.

[52]   C. Deb, F. Zhang, J. Yang, S. E. Lee, and K. W. Shah, "A review on time series forecasting techniques for building energy consumption," *Renew. Sustain. Energy Rev.*, vol. 74, pp. 902–924, Jul. 2017, doi: 10.1016/J.RSER.2017.02.085.

[53]   L. Pang, J. Zhang, M. Liu, H. Qu, and J. Wang, "Thermal Models for Avionics Pod Cabin Based on Stochastic Configuration Network (SCN)," *Energy Built Environ.*, Oct. 2019, doi: 10.1016/j.enbenv.2019.10.001.

[54]   R. Albatici and A. M. Tonelli, "Infrared thermovision technique for the assessment of thermal transmittance value of opaque building elements on site," *Energy Build.*, vol. 42, no. 11, pp. 2177–2183, Nov. 2010, doi: 10.1016/j.enbuild.2010.07.010.

[55]   Thermoworks, "Emissivity Table," 2018. https://www.thermoworks.com/emissivity_table (accessed Dec. 18, 2018).

[56]   A. Al-Habaibeh, G. Anderson, K. Damji, G. Jones, and K. Lam, "Using Infrared Thermography For Monitoring Thermal Efficiency Of Buildings -Case Studies From Nottingham Trent University," in *The 7th Jordanian International Mechanical Engineering Conference (JIMEC'7) 27*, 2010.

[57]   European Commission, "JRC Photovoltaic Geographical Information System (PVGIS) - European Commission," 2017. http://re.jrc.ec.europa.eu/pvg_tools/en/tools.html#DR (accessed Jul. 09, 2018).

[58]   time and date.com, "Past Weather in in High Wycombe, England, United Kingdom." https://www.timeanddate.com/weather/uk/high-wycombe/historic (accessed Jun. 27, 2018).

[59]   I. H. Yang, M. S. Yeo, and K. W. Kim, "Application of artificial neural network to predict the optimal start time for heating system in building," *Energy Convers. Manag.*, vol. 44, no. 17, pp. 2791–2809, Oct. 2003, doi: 10.1016/S0196-8904(03)00044-X.

[60]   J. Yang, H. Rivard, and R. Zmeureanu, "On-line building energy prediction using adaptive artificial neural networks," *Energy Build.*, vol. 37, no. 12, pp. 1250–1259, Dec. 2005, doi: 10.1016/j.enbuild.2005.02.005.

[61]   "Accolade for STYROFOAM as Greening-the-Box retrofit project wins Gold," 2012. https://www.egshpa.com/news-media/accolade-styrofoam-greening-the-box-retrofit-project-wins-gold/ (accessed Jun. 20, 2017).

[62]   Search Architects, "Working Drawings First floor plan." 2009.

[63]   Search Architects, "Working Drawings Ground floor plan." 2009.

[64]   J. Harrall, "Building Adaptation Achieves 80% Reduction In Running Costs," *Building Innovations*, Dunston, pp. 68–69, 2012.

[65]   J. Chilton and A. Al-Habaibeh, "Greening The Box^{TM} – Retrofit of Hard to Treat Housing." A Seminar Presenting an Exemplar Retrofit of a 19th century dwelling extended in the 1950s, Nottingham Trent University, 2011.

[66]   UK Power, "Gas & electricity prices per kWh - UKPower.co.uk," 2017. https://www.ukpower.co.uk/home_energy/tariffs-per-unit-kwh (accessed Sep. 13, 2017).

[67] The Sustainable Energy Association (SEA), "Wrap then Heat: A holistic strategy for making our homes and buildings healthier, cheaper and more sustainable," 2017. https://www.sustainableenergyassociation.com/wp-content/uploads/2017/03/SEA-Wrap-then-heat-digital.pdf (accessed Jan. 10, 2019).